Part B

Supported mono-copper substituted Phosphotungstate

Supports used:

i. Hydrous ZrO_2

ii. Neutral Al_2O_3

Chapter 3A

Mono-copper substituted phosphotungstate supported on Hydrous Zirconia

Synthesis, Characterization, Catalytic Evaluation and Kinetics

RSC Advances

PAPER

Cite this: *RSC Adv.*, 2019, 9, 27755

Flexible oxidation of styrene using TBHP over zirconia supported mono-copper substituted phosphotungstate

Rajesh Sadasivan and Anjali Patel *

Received 28th June 2019
Accepted 22nd August 2019

DOI: 10.1039/c9ra04892h

rsc.li/rsc-advances

A heterogeneous catalyst comprising mono-copper substituted phosphotungstate and hydrous zirconia was synthesized using wet impregnation method, characterized by various physico-chemical techniques and evaluated for solvent-free oxidation of styrene using TBHP as oxidant. Various reaction parameters like time, catalyst amount, amount of TBHP and temperature were optimized with focus on optimum selectivity of styrene-oxide. Further, the catalytic activity was compared with that of unfunctionalized $PW_{11}Cu$ to understand the role of the support. Finally, the role of each component of the reaction was clearly elucidated by a detailed kinetic study of the reaction using both the catalysts.

Amongst the different metal oxides, hydrous zirconia (ZrO_2) has shown high potential in industry as well as academia as an anti-corrosive [1], in fuel cells [2], medical implants [3], semiconductors [4] and catalysis [5], due to its outstanding properties, wear resistance, strength and biocompatibility [6]. In catalysis, especially, ZrO_2 is used not only as a catalyst in itself [7, 8], but also as a support for different catalytic materials. Extreme chemical stability and resistance to hostile chemicals, along with the ability to interact with other materials, courtesy, the surface hydroxyl groups, makes ZrO_2 an ideal support.

In this regard, there are innumerable reports on parent as well as lacunary phosphotungstates supported on to zirconia and used as catalysts for various organic transformations [9-21]. However, reports on transition metal substituted phosphotungstates supported on to zirconia are sparse. In 2004, Hu et al synthesized mono-as well as di-titanium substituted phosphotungstate and supported them on to zirconia by sol-gel technique. Various characterization techniques confirmed chemical interactions between the POM and support. Further, the synthesized materials were used as catalysts for the photo-degradation of naphthol blue black (NBB) dye to inorganic mineralized products like CO_2, NH_4^+, NO_3^-, and SO_4^{2-} [22]. More than 10 years later, in 2016, Patel et al successfully supported Cs salt of mono-nickel substituted phosphotungstate on to zirconia by wet impregnation, characterized and used for one-pot oxidative esterification of benzaldehyde using H_2O_2 as oxidant, with efficient conversion and selectivity of ester [23].

A literature survey shows that the mentioned reports are the only instances on zirconia supported transition metal substituted phosphotungstates. Further, no reports are available on mono-copper substituted phosphotungstate supported on zirconia. In the present work, we have used wet impregnation technique to support $PW_{11}Cu$ over hydrous zirconia, characterized and **evaluated** for the oxidation of alkenes using TBHP as the oxidant. Leaching and heterogeneity

tests as well as recycle studies have been carried out and finally, the kinetics of the reaction has also been studied in detail.

EXPERIMENTAL

Materials

All chemicals used were of A.R. grade. 12-tungstophosphoric acid, copper chloride dihydrate, cesium chloride, styrene, dichloromethane, 70% tert-butyl hydroperoxide, liq. NH_3 and Sodium hydroxide were obtained from Merck. Zirconium oxychloride was procured from Loba Chemie. All chemicals were used as received.

Synthesis of Zirconia

Hydrous zirconia was synthesized using a technique previously reported by our group [24]. To an aqueous solution of $ZrOCl_2.8H_2O$, ammonia solution was added drop-wise up to pH 8.5. This was aged at 100 ^{0}C for 1 h in a water bath, filtered, washed and dried at 100 ^{0}C for 10 h. the obtained material was designated ZrO_2.

Synthesis of mono-copper substituted phosphotungstate

$PW_{11}Cu$ was synthesized by the one-pot method mentioned in chapter 1.

Synthesis of mono-copper substituted phosphotungstate supported on zirconia

30% $PW_{11}Cu$ supported over zirconia was synthesized by wet impregnation method. To the aqueous solution of $PW_{11}Cu$ (0.3 g/30 mL), 1 g ZrO_2 was added, dried at 100 ^{0}C for 10 h and the resulting material was designated 30% $PW_{11}Cu/ZrO_2$. On similar lines, 10%, 20% and 40% $PW_{11}Cu/ZrO_2$ were prepared taking 0.1 g/10 mL, 0.2 g/20 mL and 0.4 g/40 mL aqueous solutions of $PW_{11}Cu$ respectively and designated as 10% $PW_{11}Cu/ZrO_2$, 20% $PW_{11}Cu/ZrO_2$ and 40% $PW_{11}Cu/ZrO_2$ respectively.

Acidity determination by potentiometry

The different types of acidic sites were determined by potentiometric titrations using n-butyl amine [25]. 0.25 g of the synthesized material was suspended in 50 mL acetonitrile and aged at 25 ^{0}C. To this, 0.1 mL of 0.05 N n-butyl amine in acetonitrile was added at regular time intervals and the potential (mV) after each addition was recorded.

Catalytic reaction

Oxidation of the styrene and cis-cyclooctene was carried out using $PW_{11}Cu/ZrO_2$ as catalyst, following the method mentioned in chapter 1.

Leaching test

Polyoxometalates can be easily characterized by a clear heteropoly blue colour when reacted with a mild reducing agent like ascorbic acid. This method was used to check for leaching of $PW_{11}Cu$ from the support.

RESULTS AND DISCUSSION

Catalyst Characterization

Absence of blue colour on reaction with ascorbic acid denoted that leaching of $PW_{11}Cu$ from ZrO_2 into the reaction medium does not take place, thereby indicating that there are strong interactions between the POM and support.

The total acidity of the synthesized materials was determined by n-butyl amine titrations and the results are presented in table 1. It can be noted that the acidity of the material decreases with increase in %loading. This may be attributed to two reasons: (i) the acidity of unsupported $PW_{11}Cu$ is very less, and as a result, loading on zirconia further suppresses the overall acidity of the material. (ii) higher loading leads to blocking of acidic sites.

Table 1. n-butyl amine acidity values

Material	Acidity (mmol n-butyl amine/g)
ZrO_2	0.62
$PW_{11}Cu$	0.5
10% $PW_{11}Cu$-ZrO_2	0.64
20% $PW_{11}Cu$-ZrO_2	0.58
30% $PW_{11}Cu$-ZrO_2	0.30
40% $PW_{11}Cu$-ZrO_2	0.22

The various acidic sites were calculated by potentiometric titration method and the acidic strength as well as total number of acidic sites are presented in table 2.

Table 2. Acidic sites determined by potentiometry

Material	Acidic strength (mV)	Types of acidic sites			Total no. of acidic sites
		Very strong	Strong	Weak	
ZrO_2	53	0	0.5	0.8	1.3
$PW_{11}Cu$	20	0	0.1	0.3	0.4
10% $PW_{11}Cu$-ZrO_2	161	0.1	0.2	1.9	2.1
20% $PW_{11}Cu$-ZrO_2	149	0.1	0.2	1.5	1.8
30% $PW_{11}Cu$-ZrO_2	140	0.1	0.1	1.0	1.2
40% $PW_{11}Cu$-ZrO_2	112	0.1	0.1	0.8	1.0

Loading of 10% $PW_{11}Cu$ on to ZrO_2, shows increase in acidity and number of acidic sites. On further increase in % loading there is a gradual decrease in total acidity as well as the total number of acidic sites. This is in good agreement with the results obtained from n-butylamine titration, which affirms that loading of $PW_{11}Cu$ on to zirconia decreases the overall acidity of the catalyst.

Further, a preliminary reaction was carried out at varied % loading of active species (10-40%) and the results are presented in figure 1. With increase in loading amount up to 30%, there is a steady increase in conversion while decrease in selectivity of benzaldehyde. This may be due to the gradual decrease in acidity with higher loading, which is in good agreement with the known fact that as acidity increases, reaction directed towards the formation of benzaldehyde via ring opening of formed epoxide.

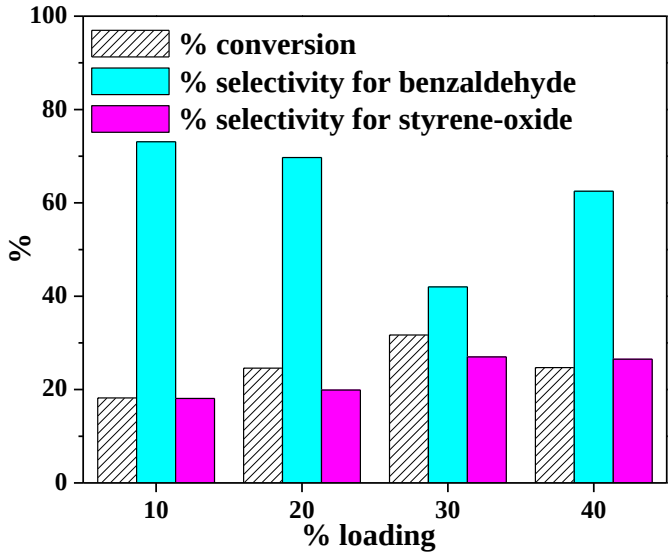

Figure 1. Effect of % loading (Catalyst amount – 25 mg; Time – 8 h; TBHP – 2 mL; Temperature – 60 ^{0}C)

Keeping in mind the importance of epoxide in the chemical industry, 30% $PW_{11}Cu/ZrO_2$ was selected and further characterizations as well as optimizations have been carried out using the same, re-designated as $PW_{11}Cu/ZrO_2$.

TGA of $PW_{11}Cu/ZrO_2$ (Figure 2) shows initial weight loss of 4.4% up to 150 ^{0}C, which is attributed to adsorbed water. Further weight loss of 7.2% is noticed between 180-350 ^{0}C because of water of crystallization. No other substantial weight loss indicates that the synthesized material is stable up to 550 ^{0}C.

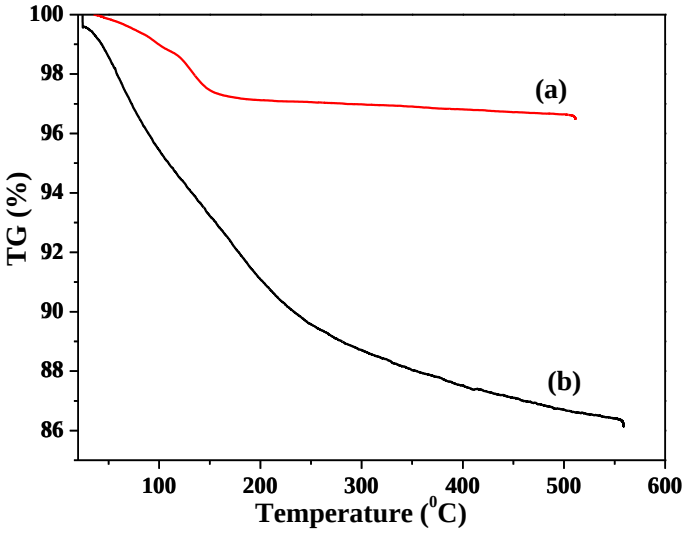

Figure 2. TGA of (a) $PW_{11}Cu$ and (b) $PW_{11}Cu/ZrO_2$

The FT-IR spectra of ZrO_2, $PW_{11}Cu$ and $PW_{11}Cu/ZrO_2$ are shown in figure 3. ZrO_2 shows bands at 3365, 1625, 1396 and 608 cm^{-1} which are characteristic of asymmetric O–H stretching, H–O–H, O–H–O bending and Zr–O–H bending vibrations respectively.

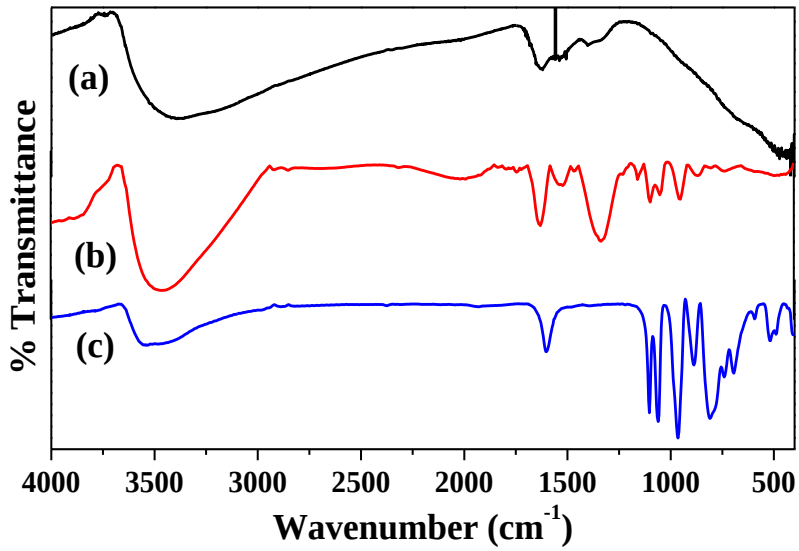

Figure 3. FT – IR spectra of (a) ZrO_2, (b) $PW_{11}Cu/ZrO_2$ and (c) $PW_{11}Cu$

$PW_{11}Cu$ exhibits bands at 1103 and 1060 cm^{-1} corresponding to P–O stretching, 964 cm^{-1} corresponding to W=O stretching, 887 and 810 cm^{-1} corresponding to W–O–W stretching and 516 cm^{-1} corresponding to Cu–O stretching vibrations respectively. The FT–IR spectrum of $PW_{11}Cu/ZrO_2$ shows characteristic bands of both $PW_{11}Cu$ and ZrO_2. Bands at 1103 and 1064 cm^{-1}; 952 cm^{-1}; and 813 cm^{-1} corresponding to P–O, W=O and W–O–W stretching vibrations are similar to $PW_{11}Cu$. In addition, broad bands at 3417, 1631 and 1402 cm^{-1} correspond to O–H stretching, H–O–H and O–H–O bending respectively are similar to that of ZrO_2. The slight shifts observed in frequencies of supported catalyst is attributed to the chemical interaction of $PW_{11}Cu$ with the support. However, the Cu–O vibration band is not visible, due to overlapping with the Zr–O–H band and hence confirmed by FT–Raman.

Figure 4 shows the FT–Raman spectra of $PW_{11}Cu$ as well as $PW_{11}Cu/ZrO_2$. It is reported that ZrO_2 shows a number of broad peaks from 100-800 cm^{-1} associated with long range amorphous state disordering [26]. The Raman spectra of $PW_{11}Cu$ shows peaks at 996 cm^{-1} corresponding to W=O symmetric stretch; 985, 215 and 153 cm^{-1} corresponding to W–O symmetric stretch; 967 and 946 cm^{-1} corresponding to W–O–W symmetric stretch respectively.

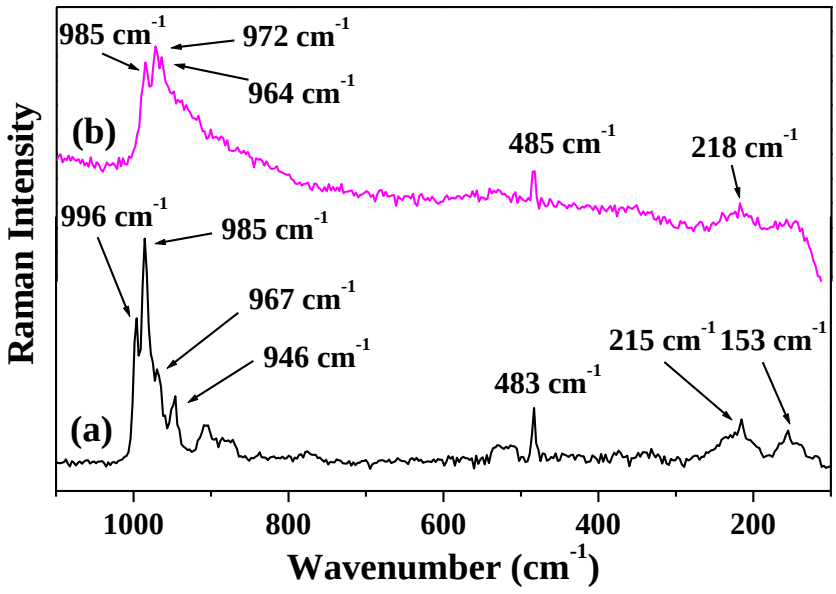

Figure 4. FT – Raman spectra of (a) $PW_{11}Cu$, (b) $PW_{11}Cu/ZrO_2$

Further, an additional peak at 483 cm^{-1} is incorporation of copper in the lacuna of PW_{11}. Similarly, Raman spectra of $PW_{11}Cu/ZrO_2$ shows peaks at 985 cm^{-1} corresponding to W=O symmetric stretch, 972 and 218 cm^{-1} corresponding to W–O symmetric stretch, and 964 cm^{-1} corresponding to W–O–W symmetric stretch respectively. A slight shift as well as decrease in intensity, along with absence of some peaks may be because of the interaction of $PW_{11}Cu$ with the support. Thus, FT–IR and FT–Raman confirm that $PW_{11}Cu$ remains intact even after impregnation on to the support.

X-Band liquid nitrogen temperature ESR spectra of unsupported $PW_{11}Cu$, ZrO_2 and $PW_{11}Cu/ZrO_2$ are presented in figure 5. As described in chapter 1, $PW_{11}Cu$ gives a four line hyperfine spectrum with g = 2.0883 and g = 2.4031, typically found in Cu(II) complexes. $PW_{11}Cu/ZrO_2$ retains the hyperfine spectrum of $PW_{11}Cu$, indicating that copper remains in +2 oxidation state and the environment around Cu(II) stays intact even after impregnation on to the support. However, the decrease in intensity observed may be due to interaction of $PW_{11}Cu$ with the support.

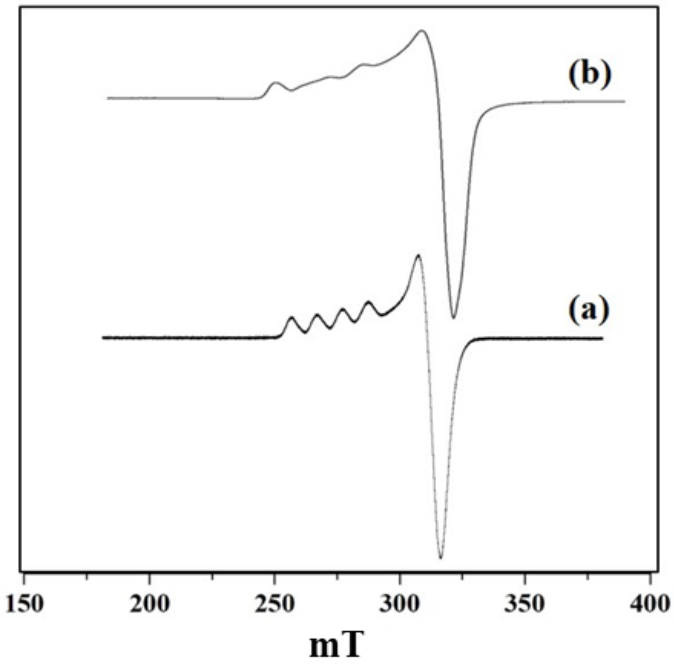

Figure 5. ESR spectra of (a) $PW_{11}Cu$ and (b) $PW_{11}Cu/ZrO_2$

The H_2-TPR spectra of $PW_{11}Cu$ and $PW_{11}Cu/ZrO_2$ are shown in figure 6. Romanelli et al obtained two peaks in the TPR pattern of sodium salt of $PW_{11}Cu$ with maxima at 666 ^{0}C and 960 ^{0}C which have been assigned to reduction of species after anion decomposition [27].

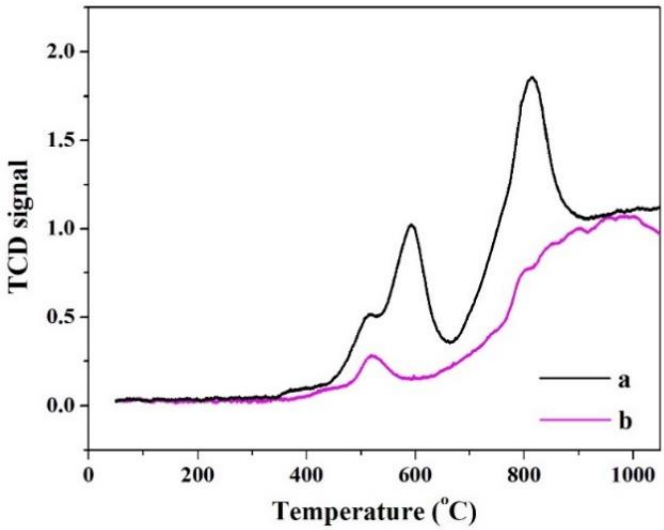

Figure 6. H_2-TPR spectra of (a) $PW_{11}Cu$ and (b) $PW_{11}Cu/ZrO_2$

In the present case, similar maxima are obtained at 592 ^{0}C and 819 ^{0}C, which is attributed to formation of WO_3 species [28]. The decrease in reduction temperature is attributed to increase in the consumption of H_2 gas due to Cs counter cation [29]. The lowering of reduction temperature may also be an indication of enhanced oxidation ability.

The H_2-TPR spectra of $PW_{11}Cu/ZrO_2$ has a peak with lesser intensity and shows maxima at 518 ^{0}C, while the second peak gets overlapped with the reduction peaks of ZrO_2, which fall in the temperature range of 700-900 ^{0}C [30]. The decrease in intensity as well as reduction temperature may be due to chemical interaction of $[PW_{11}Cu]^{5-}$ anions with the support [27]. This is further confirmed by ^{31}P MAS NMR.

^{31}P NMR is an important tool to understand the environment around phosphorus in polyoxometalates as well as the interaction of the anion with support [31]. The ^{31}P MAS NMR of $PW_{11}Cu$ and $PW_{11}Cu/ZrO_2$ are presented in

figure 7. The peak at -10.42 in case of the supported material arises because of the PO_4 unit of $PW_{11}Cu$. The slight downfield shift may be attributed to the hydrogen bonding between the terminal oxygen of the POM and –OH groups of zirconia.

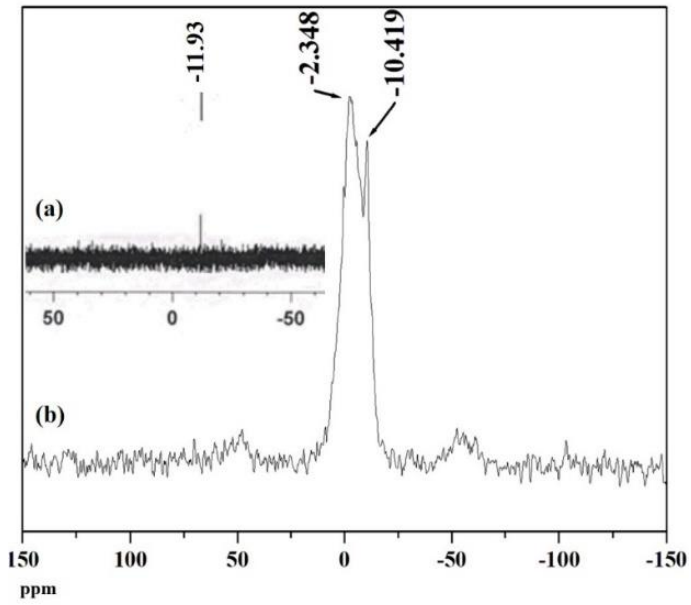

Figure 7. ^{31}P MAS NMR of (a) $PW_{11}Cu$ and (b) $PW_{11}Cu/ZrO_2$

Broad peak at -2.35 ppm is attributed to the formation of $[\equiv Zr–OH_2]^+[Cs_4(PW_{11}CuO_{39})]^-$ species [20, 22, 32]. This may be explained as follows. Loading of $PW_{11}Cu$ on to ZrO_2 is carried out by wet impregnation at 100 ^oC. Dehydration of water molecules of zirconia occurs, which is followed by subsequent entrapment of $PW_{11}Cu$ anions within the network of zirconia. Further, due to the acidic medium, ≡Zr–OH gets protonated to form $[\equiv Zr–OH_2]^+$, which acts as a cation for the anionic $(PW_{11}CuO_{39})^{5-}$ species. As a result, a chemical bond formation occurs between the two as opposed to simple physisorption. This, along with hydrogen bonding, ensures that $PW_{11}Cu$ does not leach during the catalytic reaction and the catalyst remains intact. Intensity of both the peaks in NMR indicates that while majority of $PW_{11}Cu$ form ionic pairs with zirconia, some interact only by hydrogen bonds.

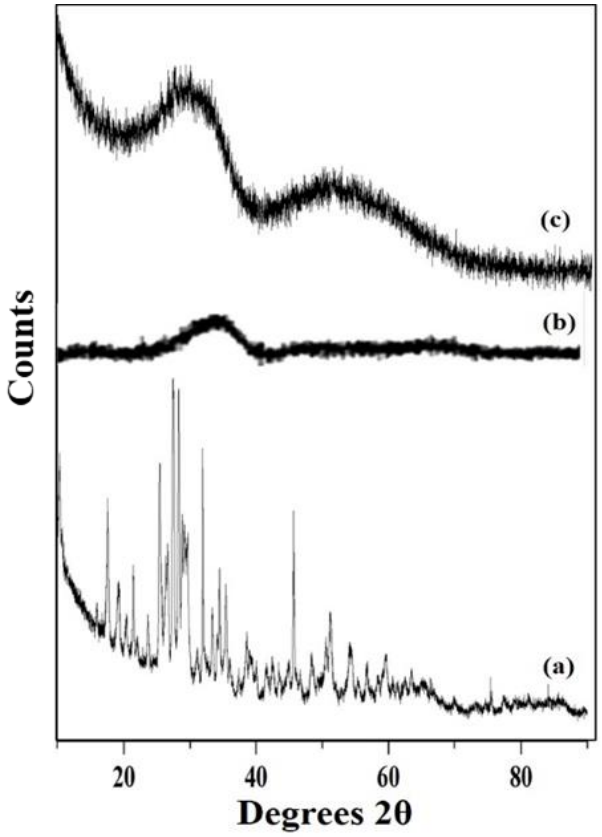

Figure 8. Wide angle powder XRD of (a) $PW_{11}Cu$, (b) ZrO_2 and (c) $PW_{11}Cu/ZrO_2$

The wide angle powder XRD of unsupported $PW_{11}Cu$, ZrO_2 and $PW_{11}Cu/ZrO_2$ are presented in figure 8. As described in chapter 1, $PW_{11}Cu$ shows sharp peaks from 20-30 degrees 2θ characteristic to the Keggin structure, with a slight shift due to incorporation of copper. This is further confirmed by sharp peaks at 48 degrees 2θ attributed to Cu(II) [33]. The absence of crystalline peaks in case of $PW_{11}Cu/ZrO_2$ indicates complete dispersion of $PW_{11}Cu$ on to the support.

The N_2 adsorption-desorption isotherms of pure ZrO_2 and $PW_{11}Cu/ZrO_2$ are shown in figure 9, and their surface area are shown in table 3. Increase in surface area of $PW_{11}Cu/ZrO_2$ (218 m^2/g) as compared to pure ZrO_2 (170 m^2/g) is attributed to supporting of $PW_{11}Cu$, which is as expected.

Table 3. BET Surface area of pure ZrO_2 and $PW_{11}Cu/ZrO_2$

Material	Surface area (m^3/g)
ZrO_2	170
$PW_{11}Cu/ZrO_2$	218

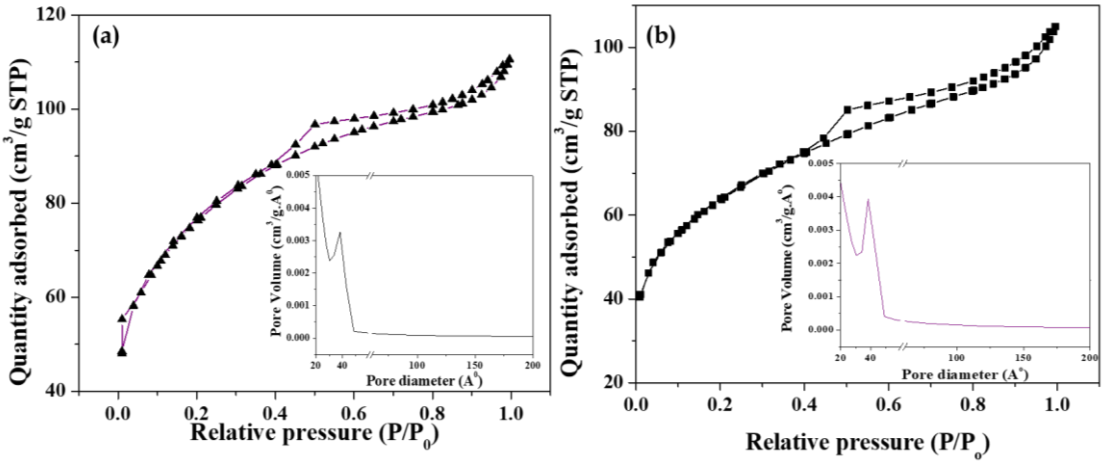

Figure 9. N_2 adsorption-desorption isotherm and (inset) pore size distribution curve of (a) pure ZrO_2 and (b) $PW_{11}Cu/ZrO_2$

Oxidation of styrene

A detailed catalytic study was carried out for the oxidation of styrene using $PW_{11}Cu/ZrO_2$ as catalyst. The reaction in the absence of the catalyst gives negligible conversion, indicating the necessity of the catalyst for oxidation reaction. Reaction parameters like % loading, reaction time, catalyst amount, amount of TBHP and reaction temperature were optimized to give maximum conversion and selectivity of desired product. The major products formed were benzaldehyde and styrene-oxide while small amounts of acetophenone and benzoic acid were formed. Small quantities of tert-butyl alcohol was formed as by-product as expected.

The effect of amount of catalyst was studied by varying the catalyst amounts (Figure 10a) and the results show that from 15 mg to 25 mg, conversion of styrene, as well as selectivity of styrene oxide increases, however, selectivity of benzaldehyde decreases. On increasing the catalyst amount to 50 mg, there is slight increase in conversion, but selectivity of styrene oxide decreases and that of benzaldehyde increases. Further increase in catalyst amount results in substantial decrease in conversion as well as selectivity of styrene-oxide, which is as expected and may be attributed to blocking of catalytic sites. Hence, 25 mg of the catalyst was considered optimum, which consisted of 6.25 mg of active $PW_{11}Cu$.

Next, reaction time was optimized (Figure 10b), and as the time is increased from 8 h to 16 h, steady increase in conversion is observed, along with selectivity of styrene-oxide. Further increase in reaction time shows no significant change in either conversion or selectivity of the required product. Therefore, reaction time was optimized at 16 h.

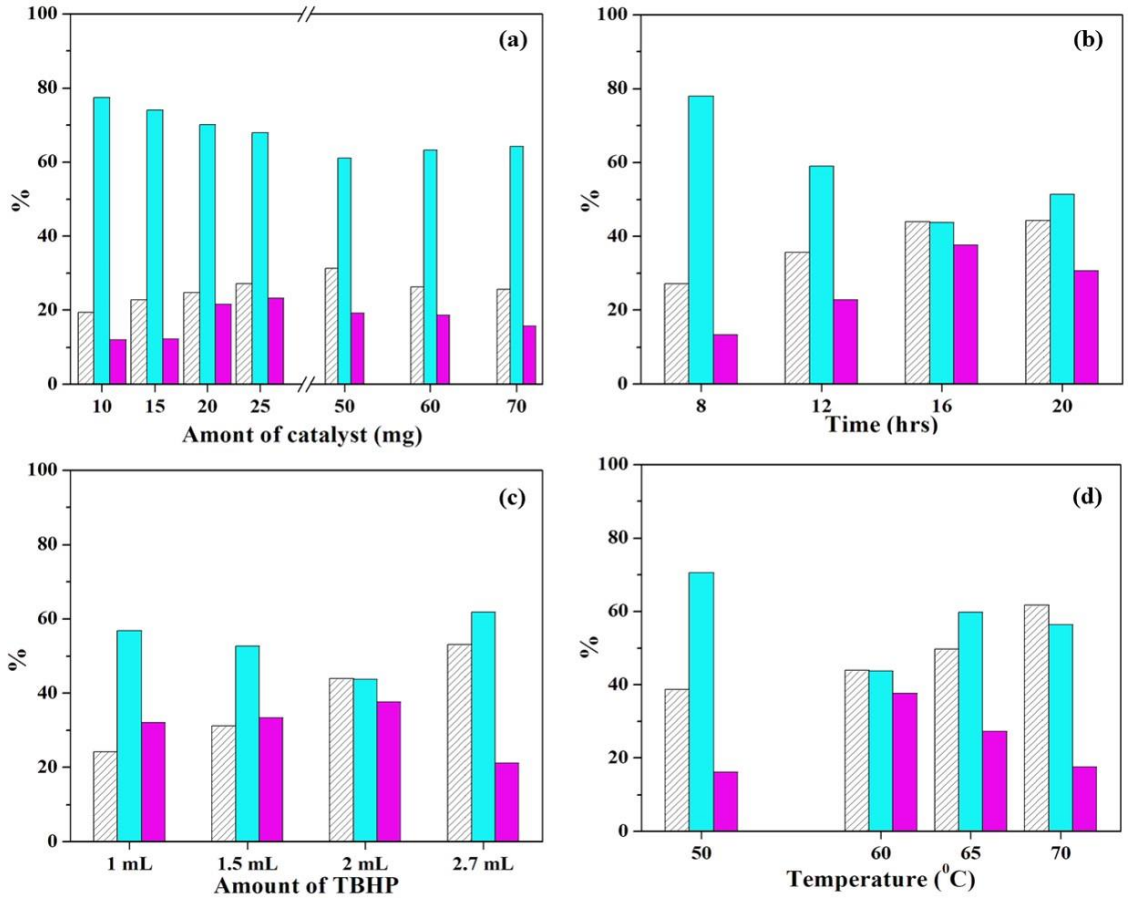

Figure 10. Optimization of parameters for oxidation of styrene (a) Effect of catalyst amount (Time – 8 h; temp – 60 ^{0}C; TBHP – 2 mL); (b) Effect of time (Catalyst amount – 25 mg; temp – 60 ^{0}C; TBHP – 2 mL); (c) Effect of amount of TBHP (catalyst amount – 25 mg; temp – 60 ^{0}C; time – 16 h); (d) Effect of temperature (catalyst amount – 25 mg; time – 16 h; TBHP – 2 mL)

The reaction was then carried out by adding different quantities of TBHP (Figure 10c) and with increase in TBHP amount from 1 mL to 2 mL, there is a steady increase in conversion of styrene, with increase in styrene-oxide selectivity and decrease in that of benzaldehyde. On further increase in TBHP amount to 2.7 mL, conversion increases, but selectivity of the epoxide decreases, with an increase in selectivity of benzaldehyde. Hence, 2 mL TBHP was considered optimum for the reaction.

Finally, the reaction temperature was optimized (Figure 10d) and on increasing the temperature from 50 ^{0}C to 60 ^{0}C, there is increase in conversion and styrene

oxide selectivity. But further increase in temperature results in significant decrease of selectivity of both epoxide as well as aldehyde, with formation of unwanted by-products in the form of polymers. This is due to decomposition of TBHP at higher temperatures. Therefore, reaction temperature was optimized at 60 ^{0}C.

The optimized conditions are as follows: catalyst amount – 25 mg (active species – 6.25 mg); reaction time – 16 h; TBHP – 2 mL; reaction temperature – 60 ^{0}C. As in previous cases, it is necessary to bring to notice that in the present systems, optimization has been carried out keeping in priority the selectivity of styrene-oxide. These conditions may be varied by the chemist depending on the requirement of the products.

Oxidation of cis-cyclooctene

Similar optimization studies were carried out for the oxidation of cis-cyclooctene using $PW_{11}Cu/ZrO_2$ as catalyst and TBHP as oxidant.

Reaction time was optimized by varying the time and with increase in time from 16 h to 24 h, steady increase in conversion was observed, while the selectivity of epoxide remained constant. Further increase in time did not show significant increase in conversion (Figure 11a). Hence, the reaction time was optimized at 24 h.

Next, the effect of amount of catalyst was studied and from 25 mg to 50 mg, a significant increase in conversion was observed. Further increase in catalyst amount resulted in decrease in conversion, attributed to blocking of active sites (Figure 11b). Hence, the catalyst amount was optimized at 50 mg, which comprised 12.5 mg of $PW_{11}Cu$.

Further, the amount of TBHP was optimized by varying the oxidant used and definite increase in conversion was observed with increase in TBHP from 1 mL to 1.5 mL. But with further increase, there is a drastic decrease in conversion and selectivity of epoxide, which is attributed to formation of unwanted by-products

due to over-oxidation (Figure 11c). Hence, 1.5 mL TBHP was taken as optimum amount.

Finally, temperature of the reaction was varied to choose the optimum reaction temperature. With increase in temperature from 50 ^{0}C to 60 ^{0}C, there is significant increase in conversion. With further increase, the conversion increases, but a drastic decrease in selectivity of epoxide (Figure 11d). Thus, 60 ^{0}C was considered optimum reaction temperature.

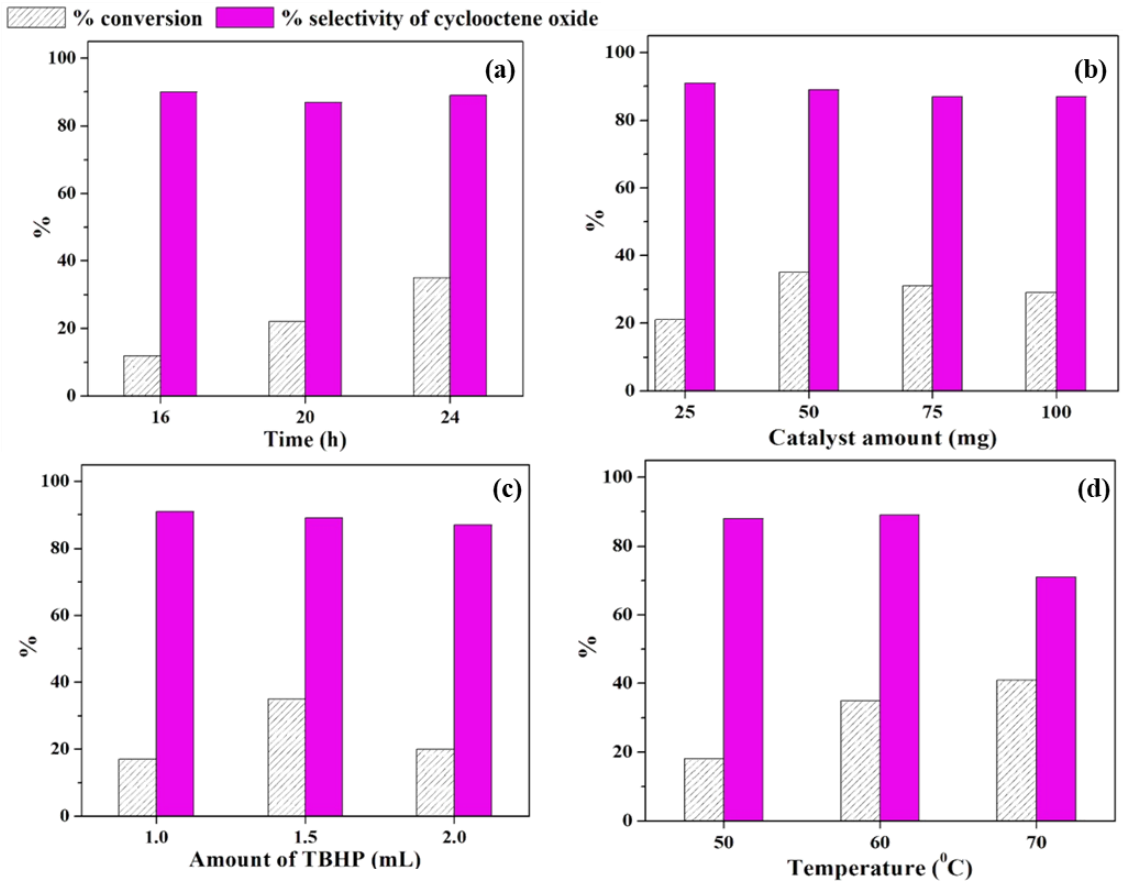

Figure 11. Optimization of parameters for oxidation of cis-cyclooctene (a) Effect of time (Catalyst amount – 50 mg; temp – 60 ^{0}C; TBHP – 1.5 mL); (b) Effect of catalyst amount (Time – 24 h; temp – 60 ^{0}C; TBHP – 1.5 mL); (c) Effect of amount of TBHP (catalyst amount – 50 mg; temp – 60 ^{0}C; time – 24 h); (d) Effect of temperature (catalyst amount – 50 mg; time – 24 h; TBHP – 1.5 mL)

The optimized conditions are as follows: catalyst amount – 50 mg (active amount of $PW_{11}Cu$ – 12.5 mg); reaction time – 24 h; TBHP – 1.5 mL and temperature – 60 ^{0}C.

Leaching and heterogeneity

Absence of blue colour on treating the reaction mixture with ascorbic acid clearly indicated that the material remains intact during the course of the reaction and $PW_{11}Cu$ does not leach out from the support.

Similar set of experiments were carried out as mentioned in chapter 1 for the study of heterogeneity of catalyst for both reactions. No change in the conversion as well as selectivity of the products (Table 4) indicates that the both catalysts are truly heterogeneous in nature.

Table 4. Heterogeneity test

Substrate	Reaction time	% conversion	% selectivity	
			Epoxide	Aldehyde/Ketone
Styrene [a]	12 h	40	44	21 / -
	16 h (Filtrate)	40	46	20 / -
Cis-cyclooctene [b]	16 h	12	90	- / 10
	20 h (Filtrate)	13	89	- / 11

[a] Catalyst amount: 25 mg; Temp: 60 ^{0}C; TBHP: 2 mL.

[b] Catalyst amount: 50 mg; Temp: 60 ^{0}C; TBHP: 1.5 mL.

Control experiments

A comparison of the activities of $PW_{11}Cu$, ZrO_2, PW_{11}/ZrO_2 and $PW_{11}Cu/ZrO_2$ for oxidation of styrene is shown in table 5. It is observed that $PW_{11}Cu/ZrO_2$ gives very high conversion along with much better selectivity of epoxide, as compared to $PW_{11}Cu$ under optimized conditions. A similar trend is observed for cis-cyclooctene, where $PW_{11}Cu/ZrO_2$ gives significantly higher conversion along with better selectivity for the epoxide compared to $PW_{11}Cu$ under optimized reaction conditions. This can be explained as follows: (i)

homogeneous dispersion of the $PW_{11}Cu$ on to ZrO_2, due to which more active sites are available for catalysis, and (ii) the overall acidity of the catalyst.

Table 5. Control experiments

Catalyst	[i] Styrene oxidation % Conv. (Ald / Epo)	[ii] Cis-cyclooctene oxidation % Conv. (Epo / Ket)	Turn Over Number (i/ii)
[b]ZrO_2	9 (83 / 10)	5 (92 / 8)	-/-
[c]$PW_{11}Cu$	21 (61 / 20)	10 (86 / 14)	1102/560
[d]PW_{11}/ZrO_2	14 (71 / 11)	6 (92 / 8)	735/336
[e]$PW_{11}Cu/ZrO_2$	44 (44 / 37)	35 (89 / 11)	2309/918

i. Styrene oxidation· Catalyst amount- [b] 18.75 mg; [c] 6.25 mg; [d] 25 mg (active amount of PW_{11}-5.95 mg); [e] 25 mg (active amount of $PW_{11}Cu$-6.25 mg); TBHP – 2 mL; Temp–60 ^{0}C; Time–16 h.

ii. Cis-cyclooctene oxidation. Catalyst amount- [a] 15 mg; [b] 37.5 mg; [c] 12.5 mg; [d] 48 mg (active amount of PW_{11} - 12 mg); [e] 50 mg (active amount of $PW_{11}Cu$ - 12.5 mg); TBHP–1.5 mL; Time–20h; Temp–65 ^{0}C

The total number of acidic sites of the support, $PW_{11}Cu$ and $PW_{11}Cu/ZrO_2$ are presented in table 6. There is a phenomenal increase in the overall acidic strength in case of supported catalyst compared to the individual materials, and hence the higher catalytic activity. This is further confirmed by a detailed kinetic study of the reaction.

Table 6. Acidic sites determined by potentiometry

Material	Acidic strength (mV)	Types of acidic sites			Total no. of acidic sites
		Very strong	Strong	Weak	
ZrO_2	53	0	0.5	0.8	1.3
$PW_{11}Cu$	20	0	0.1	0.3	0.4
$PW_{11}Cu/ZrO_2$	140	0.1	0.1	1.0	1.2

Kinetics

Experiments were carried out with different initial concentrations of the substrates and TBHP, keeping the catalyst amount constant. Equation 1 (Chapter 1) establishes a relation between the individual concentration of the reactants and time. A plot of log[(b-x)/(a-x)] versus time shows a straight line (Figure 12), indicating that the reaction is first order with respect to both the substrates and TBHP, individually [34, 35].

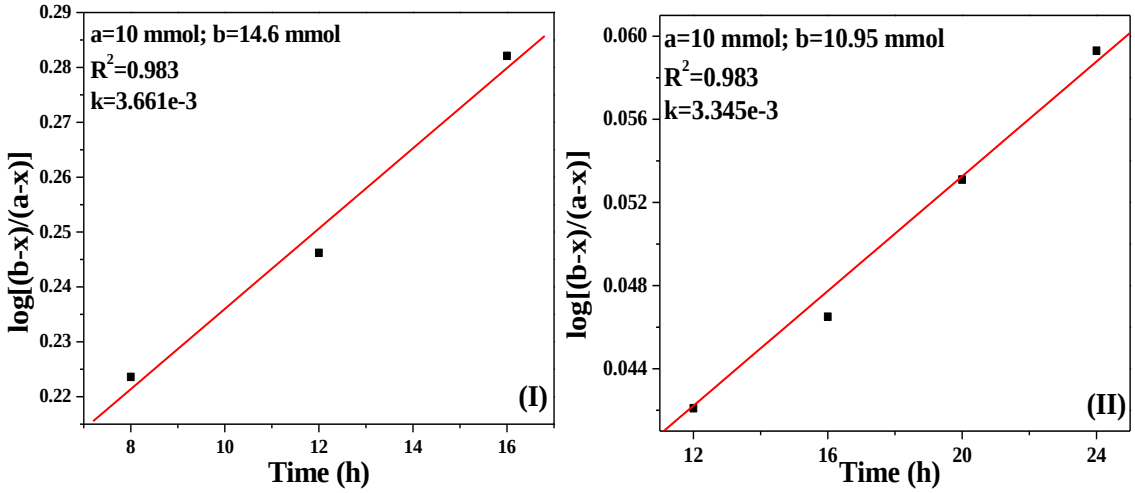

Figure 12. Plot of log[(b-x)/(a-x)] versus time for oxidation of (I) styrene and (II) cis-cyclooctene

Alternatively, an experiment was carried out with same concentration of the substrates as well as TBHP. Equation 2 (Chapter 1) establishes a relation between the concentration and time. As in the previous case, a plot of 1/(a-x) versus time shows a linear relationship in both the cases (Figure 13) indicating that the reaction follows second order overall with respect to concentration of styrene and TBHP [34, 35].

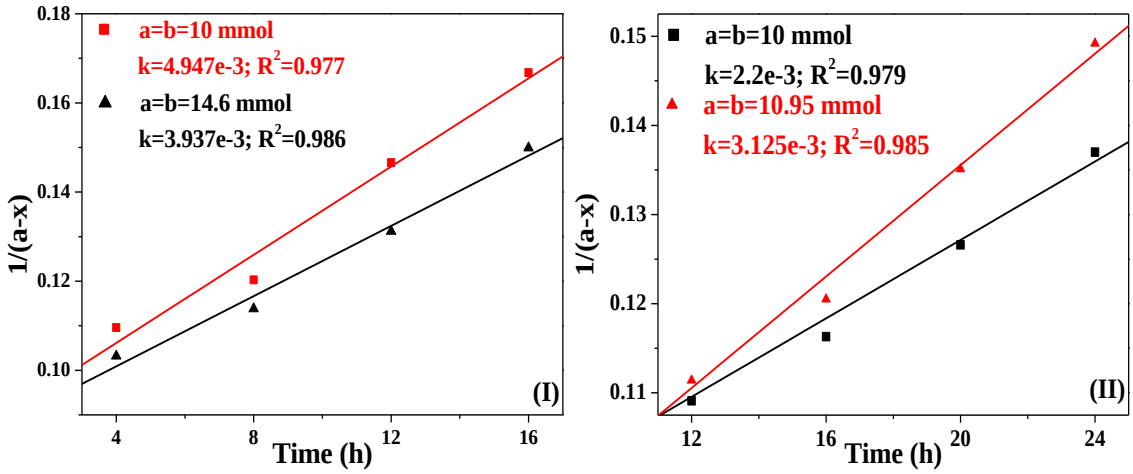

Figure 13. Plot of 1/(a-x) versus time for oxidation of (I) styrene and (II) cis-cyclooctene

The effect of reaction rate with respect to catalyst concentration was studied (Figure 14) and an increase in concentration of active species in $PW_{11}Cu/ZrO_2$ for both reactions, also shows linearity indicating that the reaction follows first order kinetics with respect to catalyst concentration [34, 35].

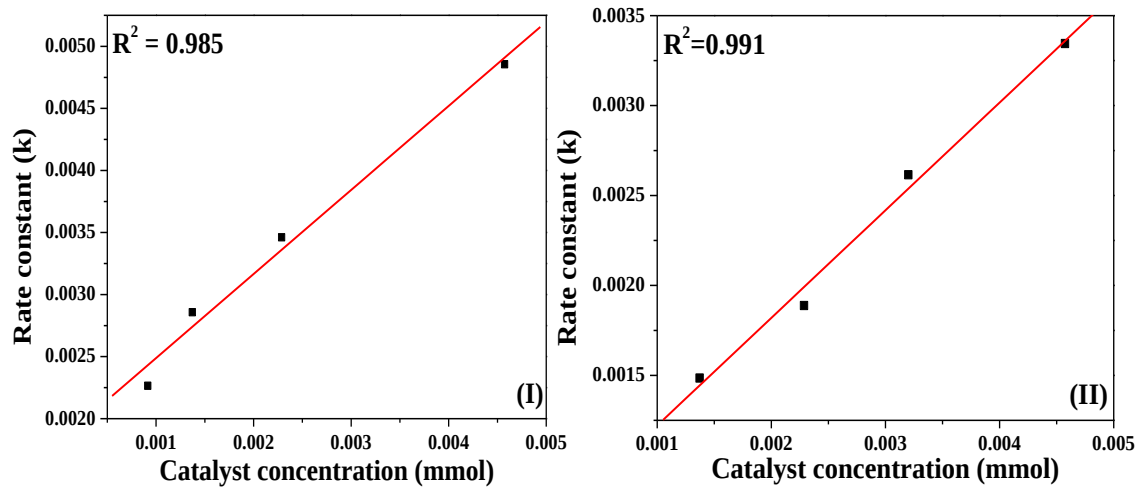

Figure 14. Plot of rate of reaction versus catalyst concentration for oxidation of (I) styrene and (II) cis-cyclooctene

Determination of Activation Energy

When temperature is increased from 323K to 353K, a gradual increase in the conversion of styrene and cis-cyclooctene is observed. Thus, 1/T shows a linear relationship with lnk (Figure 15), and the activation energy was evaluated using the Arrhenius equation (Equation 3, Chapter 1).

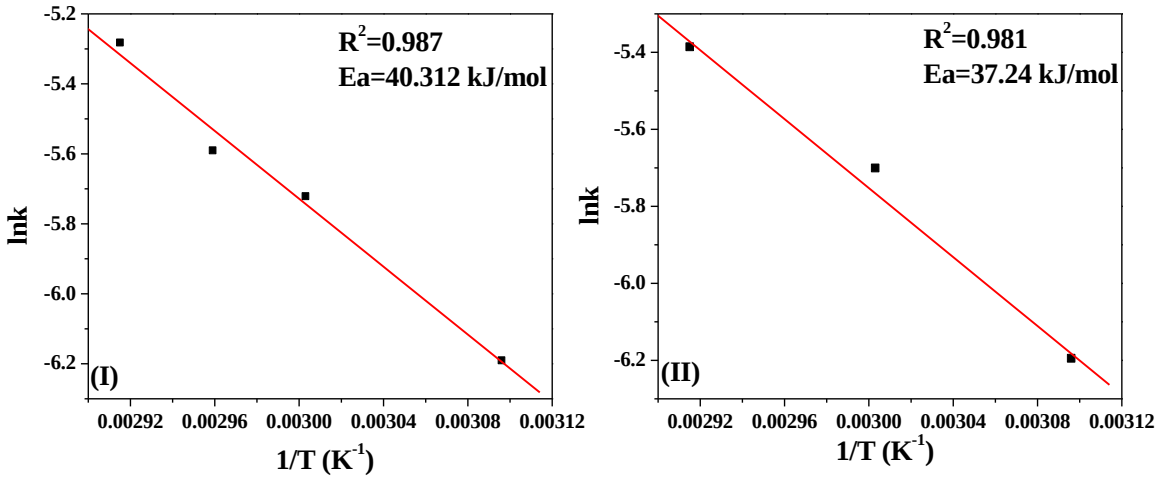

Figure 15. Plot for determination of activation energy for oxidation of (I) styrene and (II) cis-cyclooctene

Significantly higher activation energies for both reactions indicate that the reactions are truly governed by a chemical step and also that the catalyst has been exploited to its maximum capacity. Interestingly, lower activation energy of $PW_{11}Cu/ZrO_2$ compared to $PW_{11}Cu$ (Styrene oxidation: 64.81 kJ/mol; Ci-cyclooctene oxidation: 105.88 kJ/mol) also showcases the superiority of the supported system over unsupported one. Thus, the conclusions obtained from kinetic studies fittingly support that of catalysis that $PW_{11}Cu/ZrO_2$ is a better catalytic system than $PW_{11}Cu$.

Mechanistic Investigation

Mechanistic study was carried out using radial scavenger as mentioned in chapter 1 and the results for both substrates are shown in table 7. No significant change in the conversion and selectivity post addition of radical scavenger indicates that the intermediate formed is a radical and it can be assume that the reaction follows radical mechanism as described in previous chapters.

Table 7. Inhibition Experiment with 2,6-di-tert-butyl-4-methylphenol as radical scavenger

Substrate	Reaction time	% conversion	% selectivity	
			Epoxide	Aldehyde/Ketone
Styrene [a]	12 h	40	44	21
	16 h	41	44	22
Cis-cyclooctene [b]	16 h	12	90	10
	20 h	13	89	11

[a] Catalyst amount: 25 mg; temp: 60 ^{0}C; TBHP: 2 mL

[b] Catalyst amount: 50 mg; temp: 60 ^{0}C; TBHP: 1.5 mL

Recycle study

Recycle studies similar to that mentioned in chapter 1 were carried out and same conversion and selectivity for the products are obtained for both the reactions, even after multiple cycles (Table 8) indicating that the catalyst remains stable during the course of the reaction and that it can be reused for multiple times.

Table 8. Recycle study

Catalyst	% conversion	% selectivity	
		Epoxide	Aldehyde/Ketone
$PW_{11}Cu/ZrO_2$	[a]44/[b]35	[a]37/[b]89	[a]44/ [b]11
R_1-$PW_{11}Cu/ZrO_2$	[a]44/ [b]35	[a]36/ [b]89	[a]44/ [b]11
R_2-$PW_{11}Cu/ZrO_2$	[a]44/ [b]34	[a]36/ [b]90	[a]46/ [b]10
R_3-$PW_{11}Cu/ZrO_2$	[a]43/ [b]33	[a]34/ [b]89	[a]45/[b]11

[a] **Styrene oxidation**: Calyst amount: 25 mg; Temp: 60 ^{0}C; TBHP: 2 mL

[b] **Cis-cyclooctene oxidation**: Catalyst amount: 50 mg; Temp: 60 ^{0}C; TBHP: 1.5 mL

Characterization of regenerated catalyst

Regenerated $PW_{11}Cu/ZrO_2$ was characterized by FT-IR, FT–Raman, and powder XRD.

Table 9. FT - IR frequencies of fresh and recycled catalysts

Catalyst	FT-IR Frequencies (cm^{-1})						
	P-O	W=O	W-O-W	Cu-O	O–H	H–O–H	O–H–O
$PW_{11}Cu/ZrO_2$	1103 1064	952	813	-	3417	1631	1402
Rec-$PW_{11}Cu/ZrO_2$	1101 1057	960	-	-	3417	1665	1413

FT–IR of recycled $PW_{11}Cu/ZrO_2$ (Table 9) shows bands at 1101, 1057, 960 cm^{-1} corresponding to P–O and W=O frequencies, and 3417, 1665 and 1413 cm^{-1} respectively for O–H, H–O–H and O–H–O frequencies of ZrO_2. The slight decrease in the sharpness of the bands in recycled catalyst may be due to impurities that remain on the catalyst after recycling.

The FT – Raman spectra of fresh and recycled $PW_{11}Cu/ZrO_2$ (Figure 16) shows that all the characteristic peaks of the fresh catalyst are retained in the recycled one. Thus, FT – IR and FT – Raman spectra indicate that the structure remained intact even after regeneration.

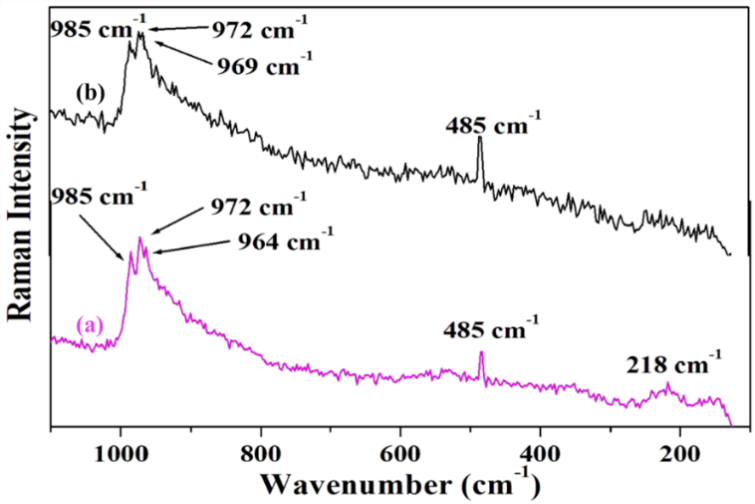

Figure 16. FT - Raman frequencies of (a) fresh and (b) recycled $PW_{11}Cu/ZrO_2$

The wide angle powder XRD patterns of fresh and recycled $PW_{11}Cu/ZrO_2$ are shown in figure 17. No appreciable change in the powder XRD of regenerated catalyst compared to the fresh one indicates that the structure remains unaffected after the regeneration of catalyst.

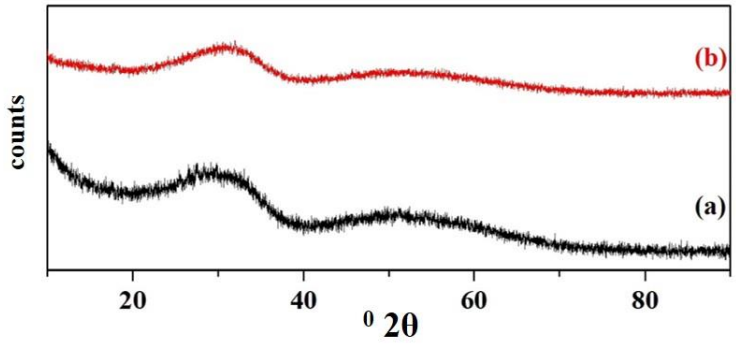

Figure 17. Wide angle powder XRD of (a) fresh and (b) regenerated $PW_{11}Cu/ZrO_2$

Comparison of substrates

Table 10. Comparison of substrates

Substrate	% conversion	% selectivity		Activation energy (Ea, kJ/mol)
		Epoxide	Aldehyde/ Ketone	
[a]Styrene	44	37	44	40.31
[b]Cis-cyclooctene	13	90	10	37.24

Catalyst amount: 25 mg; Time: 16h; temp: 60 ^{0}C; TBHP: 2 mL

Table 10 shows the comparison of the results of oxidation reaction of the two substrates. As in case of unsupported catalysts, styrene shows better reactivity compared to cis-cyclooctene and also under milder conditions. This is again because of planar morphology of styrene which is more easily activated as compared to non-planar, bulky and rigid nature of cis-cyclooctene.

Summary

- $PW_{11}Cu$ was successfully supported on to zirconia by wet impregnation technique, and reterntion of individual structures as well as chemical interations were confirmed by various spectral characterizations.
- The supported catalyst displayed better conversion as well as selectivity for epoxides for oxidation of styrene and cis-cyclooctene with lower Ea as compared to $PW_{11}Cu$, thus showcasing its superiority.
- The active species did not leach out of the support, and the catalyst exhibitted true heterogeneity under the reaction conditions.
- Further, it coud be easily recycled and reused for multiple cycles, and the characterization of regenerated catalyst confirmed retention of structure after the reaction.

References

[1] A. Yilmazbayhan, E. Breval, A. T. Motta and R. J. Comstock, J. Nucl. Mater., 3, 265-281, (2006).

[2] A. Chroneos, B. Yildiz, A. Tarancón, D. Parfitt and J. A. Kilner, Energy Environ. Sci., 8, 2774-2789, (2011).

[3] G. Wang, F. Meng, C. Ding, P. K. Chu and X. Liu, Acta Biomaterialia, 3, 990-1000, (2010).

[4] G. D. Wilk, R. M. Wallace and J. M. Anthony, J. Appl. Phys., 10, 5243-5275, (2001).

[5] C.-M. Wang, K.-N. Fan and Z.-P. Liu, J. Am. Chem. Soc., 9, 2642-2647, (2007).

[6] J. Yang, N. Zhang, H. Li, B. Xu, W. Tian and D. Dong, Polym. Int., 6, 804-810, (2015).

[7] T. Yamaguchi, Catal. Today, 2, 199-217, (1994).

[8] X. Gao, J.-M. Jehng and I. E. Wachs, J. Catal., 1, 43-50, (2002).

[9] B. M. Devassy, S. B. Halligudi, S. P. Elangovan, S. Ernst, M. Hartmann and F. Lefebvre, J. Mol. Catal. A: Chem., 1, 113-119, (2004).

[10] N. Bhatt and A. Patel, Journal of Molecular Catalysis A-chemical - J MOL CATAL A-CHEM, 223-228, (2005).

[11] B. M. Devassy, F. Lefebvre and S. B. Halligudi, J. Catal., 1, 1-10, (2005).

[12] P. Sharma and A. Patel, Bull. Mater. Sci., 5, 439, (2006).

[13] N. Bhatt, C. Shah and A. Patel, Catal. Lett., 3, 146-152, (2007).

[14] P. Shringarpure and A. Patel, Dalton Trans., 30, 3953-3955, (2008).

[15] T. Rajkumar and G. Ranga Rao, J. Mol. Catal. A: Chem., 1, 1-9, (2008).

[16] P. A. Shringarpure and A. Patel, Dalton Trans., 10, 2615-2621, (2010).

[17] C. F. Oliveira, L. M. Dezaneti, F. A. C. Garcia, J. L. de Macedo, J. A. Dias, S. C. L. Dias and K. S. P. Alvim, Appl. Catal. A: Gen, 2, 153-161, (2010).

[18] K. Li, J. Wang, Y. Zou, X. Song, H. Gao, W. Zhu, W. Zhang, J. Yu and M. Jia, Appl. Catal. A: Gen, 84-91, (2014).

[19] A. Patel and S. Singh, J. Taiwan Inst. Chem. Eng., 306-313, (2016).

[20] J. Alcañiz-Monge, B. E. Bakkali, G. Trautwein and S. Reinoso, Appl. Catal. B: Environ., 194-203, (2018).

[21] X. Liu, G. Zhao, S. Ren, G. Fang, Z. Chen and S. Li, Industrial Crops and Products, 496-504, (2018).

[22] C. Jiang, Y. Guo, C. Hu, C. Wang and D. Li, Mater. Res. Bull., 2, 251-261, (2004).

[23] A. Patel, S. Pathan and P. Prakashan, RSC Adv., 56, 51394-51402, (2016).

[24] S. Patel, N. Purohit and A. Patel, J. Mol. Catal. A: Chem., 1, 195-202, (2003).

[25] P. Vázquez, L. Pizzio, C. Cáceres, M. Blanco, H. Thomas, E. Alesso, L. Finkielsztein, B. Lantaño, G. Moltrasio and J. Aguirre, J. Mol. Catal. A: Chem., 1, 223-232, (2000).

[26] H. Wang, G. Li, Y. Xue and L. Li, J. Solid State Chem., 10, 2790-2797, (2007).

[27] R. A. Frenzel, G. P. Romanelli, M. N. Blanco and L. R. Pizzio, J. Chem. Sci., 1, 123-132, (2015).

[28] J. A. Gamelas, F. A. S. Couto, M. C. N. Trovão, A. M. V. Cavaleiro, J. A. S. Cavaleiro and J. D. P. de Jesus, Thermochim. Acta, 1, 165-173, (1999).

[29] S. Liu, L. Chen, G. Wang, J. Liu, Y. Gao, C. Li and H. Shan, Journal of Energy Chemistry, 1, 85-92, (2016).

[30] M. Shimokawabe, H. Asakawa and N. Takezawa, Appl. Catal., 1, 45-58, (1990).

[31] I. V. Kozhevnikov, K. R. Kloetstra, A. Sinnema, H. W. Zandbergen and H. van Bekkum, J. Mol. Catal. A: Chem., 1, 287-298, (1996).

[32] S. Singh and A. Patel, J. Taiwan Inst. Chem. Eng., 120-126, (2015).

[33] A. U. Patel and R. Sadasivan, ChemistrySelect, 39, 11087-11097, (2018).

[34] R. Sadasivan, A. Patel and A. Ballabh, Inorg. Chim. Acta, 345-353, (2019).

[35] Y. Liang, C. Yi, S. Tricard, J. Fang, J. Zhao and W. Shen, RSC Adv., 23, 17993-17999, (2015).

Chapter 3B

Mono-copper substituted phosphotungstate supported on Neutral Alumina

Synthesis, Characterization, Catalytic Evaluation and Kinetics

In the previous section, we have already discussed the effect of acidic support (ZrO_2) on the catalytic activity of $PW_{11}Cu$. It is well-known that heteropoly compounds cannot be supported over basic supports, as this may lead to decomposition of the same. Hence, in this section, we have attempted to study the effect of a neutral support, γ-Al_2O_3.

Numerous reports are available on Al_2O_3 supported POMs as catalysts for various applications. Most recently, Patel et al supported mono-lacunary phosphomolybdate on to alumina and used it efficiently for the oxidation of styrene as well as benzyl alcohol [1]. Kozhevnikov and his group, in 2015, supported Ni and Co-exchanged tungsto- as well as molybdophosphoric acid on to γ-Al_2O_3 and used them as a highly proficient catalysts for hydrodesulfurization reaction [2]. In the following year, Song et al immobilized sodium salt of $[\alpha\text{-}P_2W_{15}O_{56}]^{12-}$ on to alumina and used it for oxygenation of thioethers to sulfoxides [3].

Thus, a literature survey shows that despite its extensive applications, γ-Al_2O_3 has never been used to support transition metal substituted POMs. Herein for the first time, $PW_{11}Cu$ was supported on to neutral alumina by wet impregnation **its** characterization and catalytic evaluation for oxidation of styrene and cis-cyclooctene using THBP as oxidant was performed. Leaching and heterogeneity tests were carried out, as were regeneration and recycle studies. Finally a detailed kinetic study was carried out to understand the role of each component of the reaction.

EXPERIMENTAL

Materials

All chemicals used were of A.R. grade. 12-tungstophosphoric acid, Copper chloride dihydrate, Cesium chloride, styrene, dichloromethane, 70% tert-butyl hydroperoxide and neutral aluminium oxide (γ-Alumina) were obtained from Merck and were used as received.

Synthesis of undecatungstophospho(aqua) cuprate(II)

$PW_{11}Cu$ was synthesized by the one-pot technique as described in chapter 1.

Supporting of $PW_{11}Cu$ on to neutral alumina

30% $PW_{11}Cu$ was supported on to neutral alumina by wet impregnation method. 1 g γ-Al_2O_3 was added to 30% aqueous solution of $PW_{11}Cu$ (0.3 g/30 mL) and aged for 35 h at room temperature with continuous stirring. This mixture was then dried at 100 ^{0}C for 10 h and the resultant material was designated 30% $PW_{11}Cu/Al_2O_3$. On similar lines, 10%, 20% and 40% $PW_{11}Cu/Al_2O_3$ were prepared and as designated.

Acidity and acidic sites determination

The different types of acidic sites were determined by potentiometric titrations using n-butyl amine as described in chapter 3A.

Catalytic reaction

Oxidation of the alkenes was carried out using $PW_{11}Cu/Al_2O_3$ as catalyst, following the technique described in chapter 1.

Leaching of $PW_{11}Cu$ from the support was carried out following the method described in chapter 3.

RESULTS AND DISCUSSION

Catalyst characterization

Initially the catalyst was subjected to treatment with ascorbic acid solution. Absence of blue colour under warm conditions indicated that leeching of $PW_{11}Cu$ does not take place from the support. This also shows existence of strong interactions between the active species and support.

The total acidity of the synthesized materials was determined by n-butyl amine titrations and the results are presented in table 1. It can be noted that the acidity of the material decreases with increase in %loading. This may be attributed to two reasons. The acidity of unsupported $PW_{11}Cu$ is very less and with increase in loading on alumina there is steady increase in overall acidity of the material, which is as expected. Decrease in acidity value from 30% to 40% loading may be due to blocking of acidic sites as a result of higher loading.

Table 1. n-butyl amine acidity values

Material	Acidity (mmol n-butyl amine/g)
Al_2O_3	0.2
$PW_{11}Cu$	0.5
10% $PW_{11}Cu$/ Al_2O_3	0.43
20% $PW_{11}Cu$/ Al_2O_3	0.61
30% $PW_{11}Cu$/ Al_2O_3	0.83
40% $PW_{11}Cu$/ Al_2O_3	0.72

Acidic sites were calculated by potentiometric titration method and the acidic strength in terms of initial electrode potential as well as total number of acidic sites are presented in Table 2. Alumina shows negative acidity and negligible acidic sites because of its neutral nature. Similarly, the acidity of $PW_{11}Cu$ is also very less. However, supporting $PW_{11}Cu$ on to alumina increases the overall acidity as well as acidic strength of the catalyst to a great extent, which is

expected. However, the acidic strength for 40% loaded catalyst is significantly lesser that that of 30% loaded one, despite its higher acidic sites. This is attributed to blocking of catalytic sites and is in good agreement with the results obtained from n-butylamine titration. Thus, from the acidity determination by n-butylamine titration as well as by potentiometry, 30% loading was found to be optimum.

Table 2. Acidic strength and acidic sites determined by potentiometry

Material	Acidic strength (mV)	Types of acidic sites			Total no. of acidic sites
		Very strong	Strong	Weak	
Al_2O_3	-30	0	0	0.1	0.1
$PW_{11}Cu$	20	0	0.1	0.3	0.4
10% $PW_{11}Cu$/ Al_2O_3	62	0	0.1	0.4	0.5
20% $PW_{11}Cu$/ Al_2O_3	88	0	0.1	0.9	1.0
30% $PW_{11}Cu$/ Al_2O_3	113	0.1	0.1	1.3	1.5
40% $PW_{11}Cu$/ Al_2O_3	83	0	0.1	1.7	1.8

In order to optimize the amount of loading, preliminary reaction was carried out for the oxidation of styrene varying the % loading of $PW_{11}Cu$ (Figure 1). A steady increase in conversion along with high selectivity for benzaldehyde is seen from 10% - 30% loading which is expected because of the increasing acidity of the catalyst. With further increase in loading there is drastic decrease in the conversion, attributed to blocking of catalytic sites and also confirming the observations of acidity experiments. Hence, 30% loading was considered optimum and further characterization and catalytic activity were carried out with 30% $PW_{11}Cu/Al_2O_3$, re-designated as $PW_{11}Cu/Al_2O_3$.

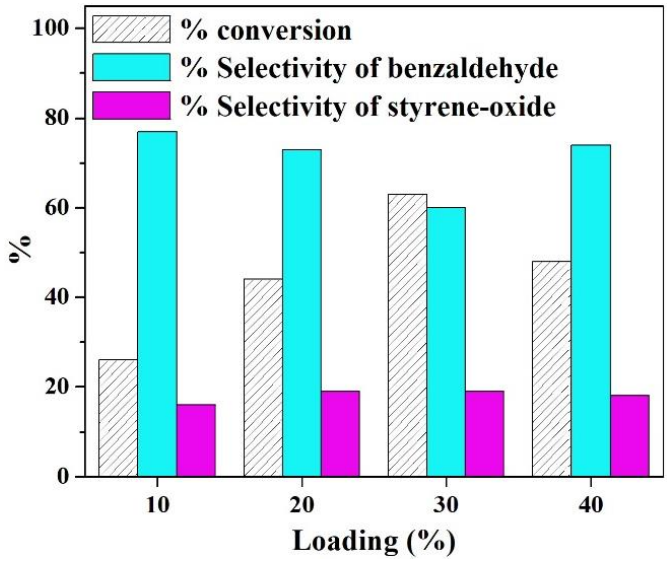

Figure 1. Effect of % loading (Catalyst amount - 25 mg; Time – 16 h; TBHP - 2 mL; Temperature - 60 ^{0}C)

TGA of $PW_{11}Cu$ and $PW_{11}Cu/Al_2O_3$ are shown in figure 2. The TGA of $PW_{11}Cu/Al_2O_3$ shows an initial weight loss of 2.1% up to 150 ^{0}C attributed to loss of adsorbed water molecules. Further, weight loss of 5.3% between 180 - 450 ^{0}C may be due to loss of crystallization water molecules. No further loss is observed indicating that the synthesized material remains stable up to 500 ^{0}C.

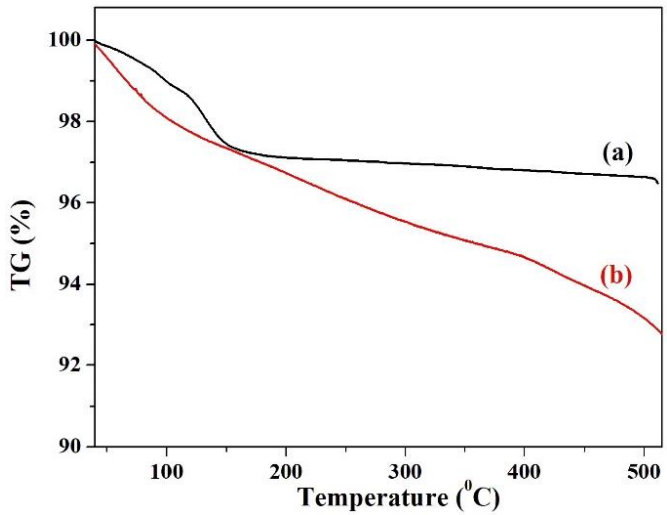

Figure 2. TGA of (a) $PW_{11}Cu$ and (b) $PW_{11}Cu/Al_2O_3$

The FT–IR spectra of Al_2O_3, $PW_{11}Cu/Al_2O_3$ and $PW_{11}Cu$ are shown in figure 3. Alumina shows characteristic bands at 3365, 1625 and 1396 cm^{-1} corresponding

to O–H, H–O–H and O–H–O stretching vibrations respectively. Further, broad bands between 1000-400 cm^{-1} correspond to the various Al–O vibrations. Band around 900 cm^{-1} corresponds to Al–O–Al stretching vibrations while a band at 763 cm^{-1} corresponds to Al–O stretching vibrations and the peaks between 700-500 cm^{-1} are assigned to AlO_6 vibrations [4, 5].

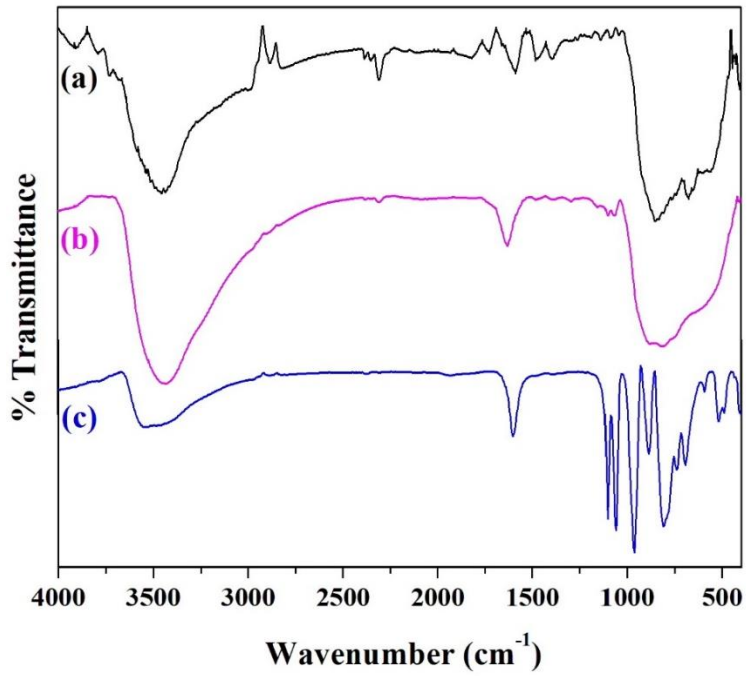

Figure 3. FT - IR spectra of (a) Al_2O_3, (b) $PW_{11}Cu/Al_2O_3$ and (c) $PW_{11}Cu$

$PW_{11}Cu$ shows characteristic bands at 1103 and 1061, 964, 887 and 810 cm^{-1} corresponding to P–O, W=O and W–O–W stretching vibrations respectively. Apart from this, the band obtained at 489 cm^{-1} corresponds to Cu–O frequency. $PW_{11}Cu/Al_2O_3$ shows bands at 1099 and 1064 cm^{-1} corresponding to P–O stretching vibrations of $PW_{11}Cu$. Apart from this, bands at 3437 and 1627 cm^{-1} corresponding to O–H and H–O–H vibrations of Al_2O_3 are also observed. The bands of $PW_{11}Cu$ between 900-500 cm^{-1} are not visible due to overlapping with bands belonging to Al_2O_3. Slight shift in the bands along with absence of some bands in case of $PW_{11}Cu/Al_2O_3$ may be due to chemical interactions between $PW_{11}Cu$ and the support.

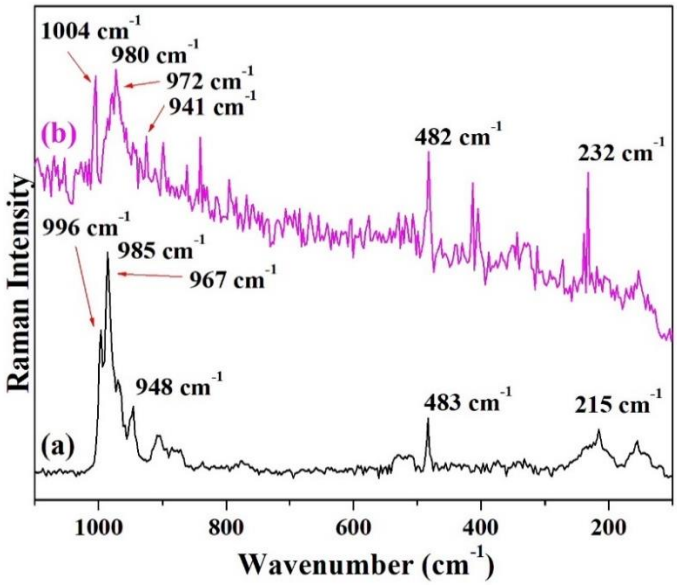

Figure 4. FT – Raman spectra of (a) $PW_{11}Cu$ and (b) $PW_{11}Cu/Al_2O_3$

Figure 4 shows the FT-Raman spectra of $PW_{11}Cu$ and $PW_{11}Cu/Al_2O_3$. Characteristic bands at 996 cm^{-1}, 985 and 215 cm^{-1}, 967 and 946 cm^{-1} corresponding to W=O symmetric stretch, W–O symmetric stretch and W–O–W symmetric stretch respectively are observed in case of $PW_{11}Cu$ along with an additional band at 483 cm^{-1} corresponding to Cu–O symmetric stretch. Similar bands are observed in case of $PW_{11}Cu/Al_2O_3$ indicating that the Keggin unit remains intact even after supporting. A slight shift in case of supported material indicates the successful supporting of $PW_{11}Cu$ on to Al_2O_3 via chemical interactions.

Figure 5 shows the H_2-TPR spectra of $PW_{11}Cu$ and $PW_{11}Cu/Al_2O_3$. As explained in chapter 3, $PW_{11}Cu$ shows maxima at 592 ^0C and 819 ^0C corresponding to formation of WO_3 species after decomposition of anion. The decrease in reduction temperature compared to reported ones is attributed to presence of Cs counter-cation, which leads to increase in consumption of H_2 gas.

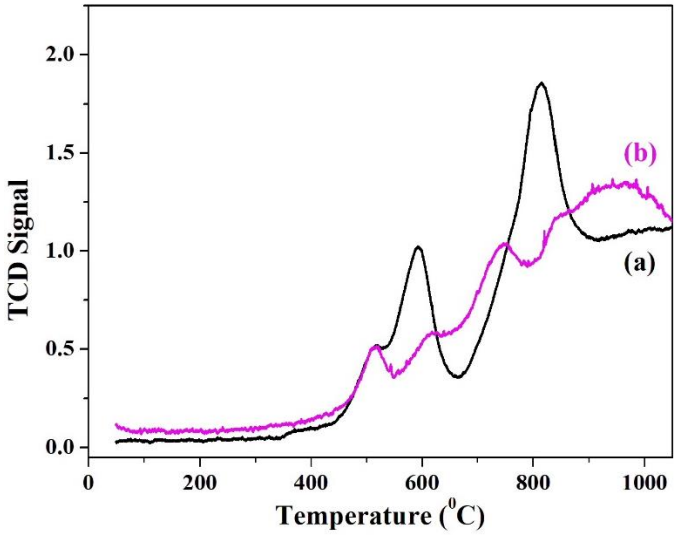

Figure 5. H_2-TPR spectra of (a) $PW_{11}Cu$ and (b) $PW_{11}Cu/Al_2O_3$

The H_2-TPR spectrum of $PW_{11}Cu/Al_2O_3$ shows two maxima at 522 ^{0}C and 750 ^{0}C like in case of $PW_{11}Cu$. Along with this, broad peaks are observed at temperatures above 800 ^{0}C corresponding to the reduction of alumina. The decrease in the intensity as well as reduction temperatures of $PW_{11}Cu$ in the supported material is attributed to strong chemical interactions between the active species and the support.

^{31}P MAS NMR studies were carried out to understand the changes in the environment around phosphorus after supporting and also the interactions of the POM with support. $PW_{11}Cu/Al_2O_3$ shows a single peak at 6.01 ppm, which is downfield compared to unsupported $PW_{11}Cu$ (-11.82 ppm) (Figure 6). This downfield shift is attributed to two reasons. Firstly, some water molecules of $PW_{11}Cu$ are lost when they are immobilized on to the support during impregnation [6]. Secondly, the existence of strong chemical interactions between $PW_{11}Cu$ and Al_2O_3, as indicated in previous studies. The acidity of the medium caused by the POM results in the dehydroxylation of surface –O–H groups of alumina to give rise to electron donor and acceptor sites. These interact with the protons of water molecules of $PW_{11}Cu$ thereby resulting in an overall negative charge over the Keggin unit. The negatively charged Keggin anions bind with the protonated support via electrostatic interactions and form strong

chemical bonds also ensuring that $PW_{11}Cu$ does not leach out from the support [7]. Similar type of interactions are also observed in case of other supports like SiO_2 and ZrO_2.

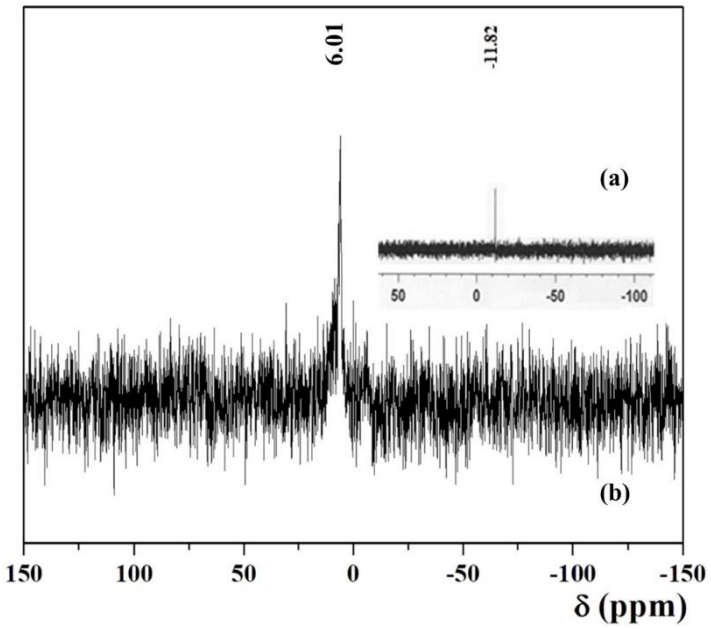

Figure 6. ^{31}P MAS NMR of (a) $PW_{11}Cu$ and (b) $PW_{11}Cu/Al_2O_3$

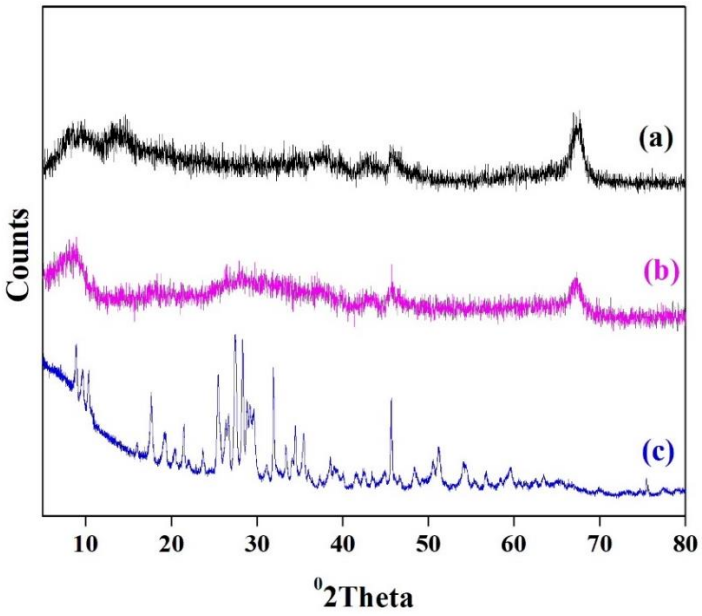

Figure 7. Powder XRD spectra of (a) Al_2O_3, (b) $PW_{11}Cu/Al_2O_3$ and (c) $PW_{11}Cu$

Figure 7 shows the wide angle powder XRD patterns of alumina and $PW_{11}Cu/Al_2O_3$. Alumina shows reflection peaks at 37^0, 48^0 and 66^0 2θ

corresponding to 311, 400 and 440 reflection planes, which are in good agreement with reported work [7]. Powder XRD patterns of $PW_{11}Cu$ show sharp crystalline peaks between 20^0-30^0 2θ, which have been explained in chapter 1. In case of $PW_{11}Cu/Al_2O_3$, the sharp peaks disappear indicating homogeneous dispersion of $PW_{11}Cu$ over the support.

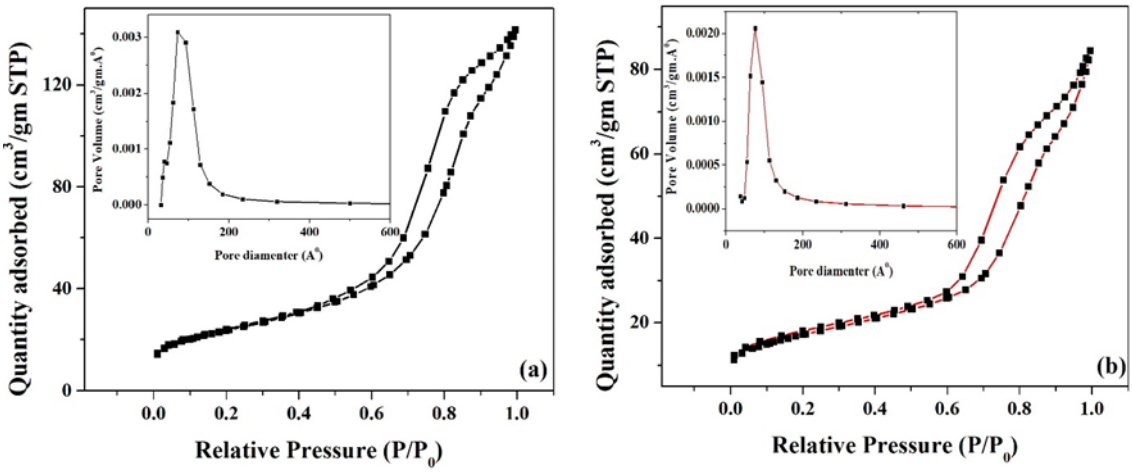

Figure 8. N_2 sorption curves and (inset) average pore diameters of (a) Al_2O_3 and (b) $PW_{11}Cu/Al_2O_3$

BET surface area of Al_2O_3 and $PW_{11}Cu/Al_2O_3$ are shown in table 3 and the isotherms are shown in figure 8. There is decrease in surface area of the supported material because of incorporation of $PW_{11}Cu$ on to the support which is in agreement with the reported results [3]. This is attributed to the fact that oxide supported catalysts tend to show decrease because of strong chemical interactions between the support and active species [8]. From the pore size distribution curve, the average pore diameter of the supported material was found to be 88 A^0.

Table 3. BET Surface area of Al_2O_3 and $PW_{11}Cu/Al_2O_3$

Material	Surface area (m^2/g)	Pore diameter (A^0)
Al_2O_3	83	105
$PW_{11}Cu/Al_2O_3$	59	88

Oxidation of styrene

The synthesized material was evaluated for its catalytic activity for the oxidation of styrene using TBHP as oxidant. Various reaction parameters like catalyst amount, reaction time, amount of TBHP as well as temperature were optimized for best possible conversion and selectivity of desired product.

The effect of catalyst amount was first studied (Figure 9) and on increase of catalyst amount from 10 mg to 25 mg, there is a steady increase in the conversion as well as selectivity of benzaldehyde, with a decrease in selectivity of styrene-oxide. This is expected because overall acidity of the system will increase with increase in catalyst amount. On further increase of catalyst amount, there is a decrease in the conversion and this is attributed to blocking of catalytic sites. Hence, 25 mg was considered optimum amount for the reaction.

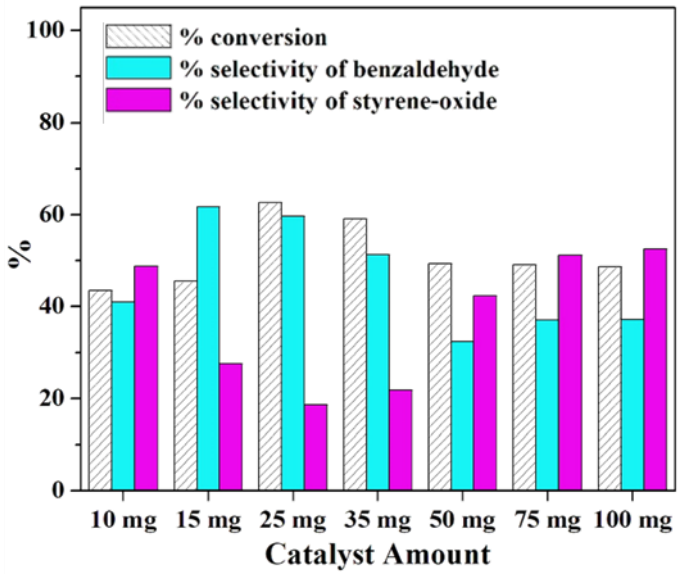

Figure 9. Effect of catalyst amount (Time –16 h; temp – 60 ^{0}C; TBHP – 2 mL)

Next, the reaction time was varied (Figure 10) and with increase in time from 4 h to 16 h, conversion increases. However, initially the selectivity of benzaldehyde decreases with increase in styrene-oxide selectivity and then both become constant, which is as expected. Beyond 16 h, there is negligible increase in the conversion and hence 16 h was considered optimum.

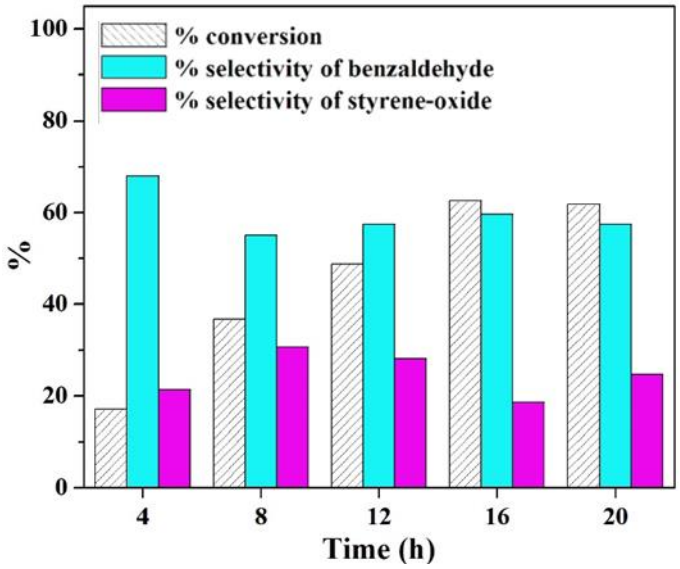

Figure 10. Effect of time (Catalyst amount – 25 mg; temp – 60 ^{0}C; TBHP – 2 mL)

TBHP amount was increased from 1 mL to 2 mL, and a steady increase in conversion of styrene is observed while the selectivity for benzaldehyde remains more or less constant. On further increase in TBHP amount to 2.7 mL, there is a drastic decrease in conversion as well as selectivity of desired products (Figure 11). Hence, 2 mL TBHP was considered optimum for the reaction.

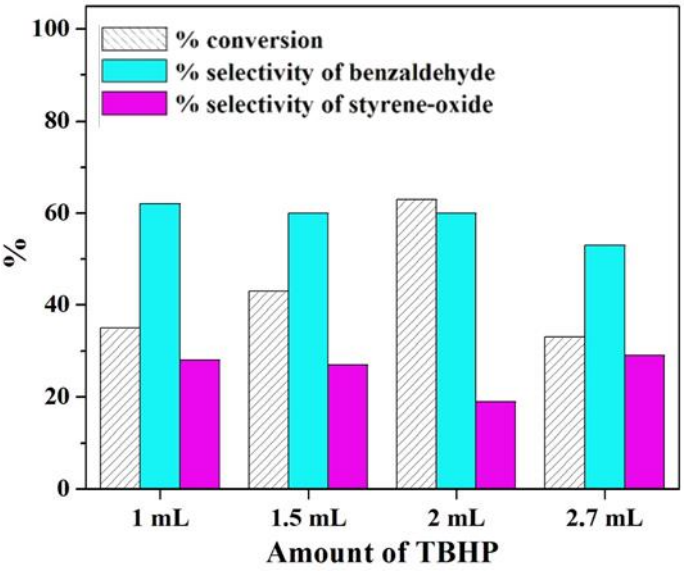

Figure 11. Effect of TBHP amount (catalyst amount – 25 mg; temp – 60 ^{0}C; time – 16 h)

Finally, the reaction was carried at different temperatures and the results are presented in figure 12. When the temperature was increased from 50 ^{0}C to 60 ^{0}C, there is an increase in conversion as well as selectivity of benzaldehyde. But on increasing temperature beyond 60 ^{0}C, there is a significant decrease in the selectivity and formation of unwanted by-products due to the degradation of TBHP at higher temperatures. Hence, temperature was optimized at 60 ^{0}C.

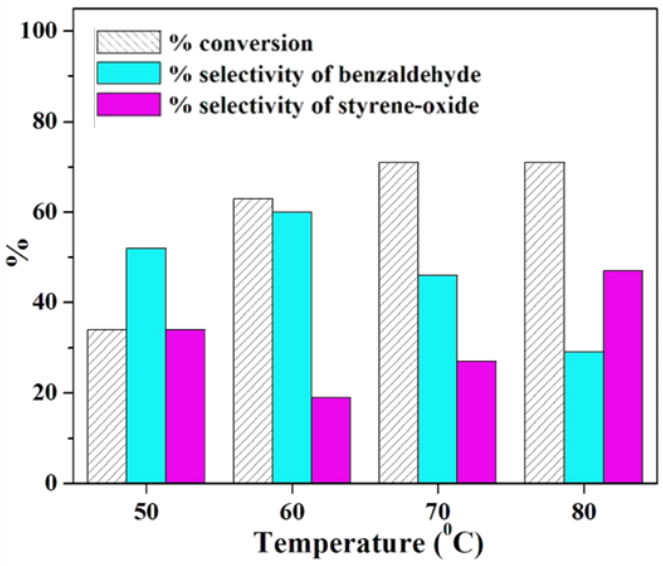

Figure 12. Effect of reaction temperature (catalyst amount – 25 mg; time – 16 h; TBHP – 2 mL)

The optimized conditions are as follows: catalyst amount – 25 mg (active species – 6.25 mg); reaction time – 16 h; TBHP – 2 mL; reaction temperature – 60 ^{0}C for 63% conversion, 60% selectivity of benzaldehyde and 19% selectivity of styrene-oxide. As in previous cases, it is necessary to bring to notice that in the present systems, optimization has been carried out keeping in priority the better selectivity of benzaldehyde. These conditions may be varied depending on the requirement of the products.

Oxidation of cis-cyclooctene

Similar experiments were carried out for oxidation of cis-cyclooctene using TBHP as oxidant. Experiments with varied amounts of the catalyst (Table 4) showed very poor conversion even at moderate to high catalyst amounts.

Table 4. Oxidation of cis-cyclooctene - varying catalyst amount

Catalyst Amount	% Conversion	% Selectivity	
		Cyclooctene-oxide	Cyclooctanone
15 mg	9.8	88	12
25 mg	10	91	9
35 mg	12	93	7
50 mg	13.5	90	10
75 mg	14.7	87	13
100 mg	14	88	12

Time: 20 h Temp: 60 ^{0}C; TBHP: 2 mL

In another attempt to increase conversion, the reaction was carried out varying the time (Table 5). Here too, the results showed very poor conversions up to 24 h. Hence, it was decided not to carry forward with the present system.

Table 5. Oxidation of cis-cyclooctene - varying catalyst amount

Time	% Conversion	% Selectivity	
		Cyclooctene-oxide	Cyclooctanone
10 h	**8**	**89**	**11**
12 h	**11**	**90**	**10**
16 h	**13**	**90**	**10**
20 h	**14**	**90**	**10**
24 h	**14**	**88**	**12**

Catalyst amount: 50 mg (Active amount of $PW_{11}Cu$ – 12.5 mg); Temp: 60 ^{0}C; TBHP: 2 mL

It is well known that cyclic alkenes are highly electron rich while terminal alkenes are comparitively electron poor [9]. Hence, the more nucleophilic cyclooctene gets adsorbed on the surface of the catalyst, which does not allow it to desorb for the reaction to occur. Therefore, though $PW_{11}Cu/Al_2O_3$ is the better catalyst for styrene oxidation, oxidation of cis-cyclooctene is not feasible over the same.

Leaching and heterogeneity

Leaching test was carried out as described previously, and absence of blue colour confirmed that $PW_{11}Cu$ does not leach out from the support.

Similarly, heterogeneity test was performed as described in previous chapter and results are presented in table 6. No change was observed in the conversion as well as selectivity of the products, indicating that the catalyst is truly heterogeneous in nature.

Table 6. Heterogeneity test

Reaction time	% conversion	% selectivity	
		Styrene-oxide	Benzaldehyde
12 h	49	28	58
16 h (Filtrate)	49	28	59

Catalyst amount-25 mg; TBHP – 2 mL; Temperature–60 ^{0}C

Control Experiments

In order to understand the role of support, the reaction was carried out using the active amount of $PW_{11}Cu$ present in the catalyst under optimized conditions, as well as only the support, and the results are presented in table 7. It can be seen that the supported catalyst gives three times the conversion as that of unsupported one. This is attributed to two reasons as described in chapter 3A: higher acidity of supported catalyst and homogeneous dispersion of active species on the support, due to which more number of active species are available for the reaction.

Table 7. Control Experiments

Catalyst	% conversion	% selectivity		Turn Over Number (TON)
		Styrene-oxide	Benzaldehyde	
[a] Al_2O_3	-	-	-	-
[b] $PW_{11}Cu$	21	20	67	1102
[c] PW_{11}/Al_2O_3	13	8	83	-
[d] $PW_{11}Cu/Al_2O_3$	63	19	60	3306

Catalyst amount- [a] 19.75 mg; [b] 6.25 mg; [c] 20 mg (active amount of PW_{11}-6 mg); [d] 25 mg (active amount of $PW_{11}Cu$-6.25 mg); TBHP – 2 mL; Temp–60 ^{0}C; Time–16h;

Further, as mentioned in chapter 3A, higher acidity of the supported material compared to unsupported one as well as the support also results in higher catalytic activity. The total number of acidic sites of the support, $PW_{11}Cu$ and $PW_{11}Cu/Al_2O_3$ were calculated by potentiometry and the results are presented in table 8.

Table 8. Acidic strength and acidic sites determined by potentiometry

Material	Acidic strength (mV)	Types of acidic sites			Total no. of acidic sites
		Very strong	Strong	Weak	
Al_2O_3	-30	0	0	0.1	0.1
$PW_{11}Cu$	20	0	0.1	0.3	0.4
$PW_{11}Cu/Al_2O_3$	113	0.1	0.1	1.3	1.5

Kinetics

Experiments were carried out to obtain the rate and determine the order of reaction, and also the activation energy of the reaction, similar to previous chapters.

Experiments were carried out with different initial concentrations of styrene and TBHP, keeping the catalyst amount constant. Equation 1 (Chapter 1) gives a

relation between the individual concentration of the reactants and time where 'a' is the initial concentration of styrene, 'b' is the initial concentration of TBHP and 'x' is the concentration at time t. A plot of log[(b-x)/(a-x)] versus time shows a straight line (Figure 13) indicating that, the reaction follows first order kinetics with respect to styrene and TBHP, individually [10, 11].

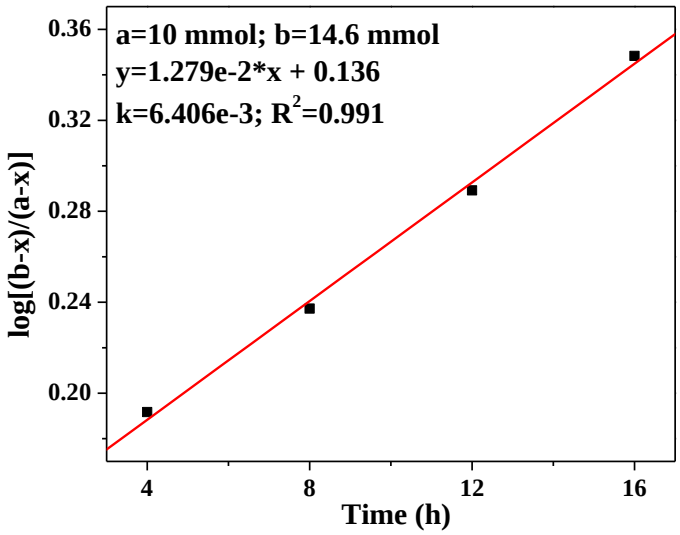

Figure 13. Plot of log[(b-x)/(a-x)] versus time

Further, an experiment was then carried out keeping the concentration of styrene as well as TBHP the same. Equation 2 (Chapter 1) establishes a relation between the concentration and time, where 'a' is the initial concentrations of styrene and TBHP and 'x' is the conversion of styrene at time t. A plot of 1/(a-x) versus time shows a linear relationship (Figure 14) indicating that the reaction follows second order kinetics with respect to concentration of styrene and TBHP overall [10, 11].

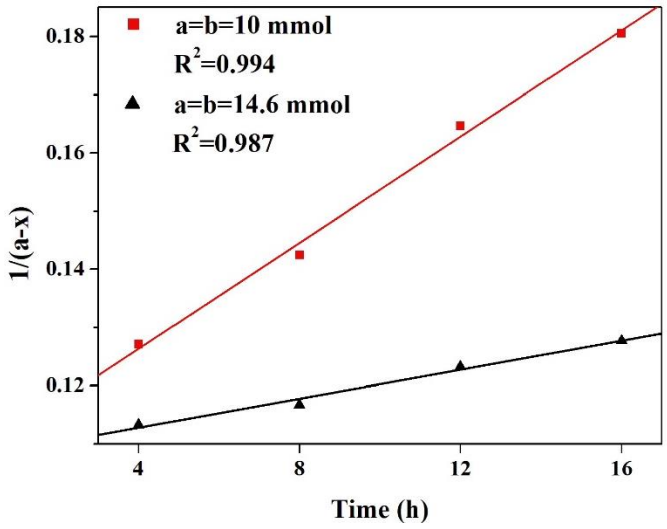

Figure 14. Plot of 1/(a-x) versus time

The effect of rate of reaction with respect to concentration of catalyst was studied by carrying out the reaction at different catalyst concentrations. A plot of catalyst concentration versus rate constant gave a straight line (Figure 15), thereby indicating that the reaction follows first order with respect to catalyst concentration as well [10, 11].

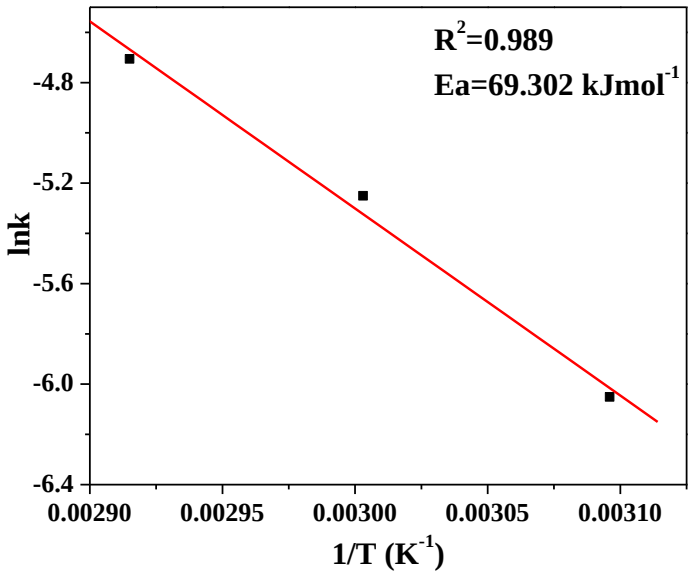

Figure 15. Plot of rate of reaction versus catalyst concentration

Determination of Activation Energy

A gradual increase in reaction rate is observed with increase in temperature from 333K to 353K and a plot of 1/T versus lnk shows linearity (Figure 16). Based on this, the activation energy of the reaction was obtained using Arrhenius equation. Significantly higher activation energy of 69.302 kJ/mol indicates that the reaction is truly governed by a chemical step and also that the catalyst has been exploited to its maximum capacity.

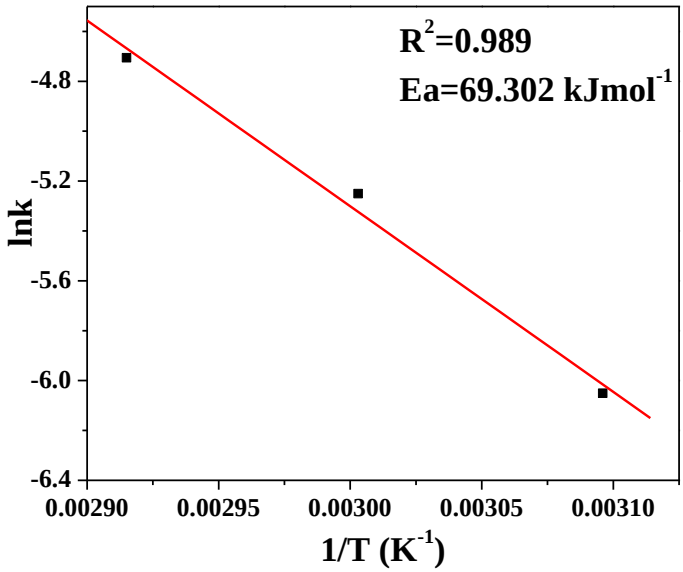

Figure 16. Plot for determination of activation energy

Mechanistic Investigation

As described in chapter 1, radical scavenger experiment was carried out for mechanistic investigations (Table 9). Similar results indicated that the reaction follows radical mechanism as described in Chapters 1 and 2.

Table 9. Inhibition Experiment with 2,6-di-tert-butyl-4-methylphenol as radical scavenger

Condition	% conversion	% selectivity	
		Benzaldehyde	Styrene-oxide
After 12 h	49	58	28
After 16 h (after scavenger addition)	50	60	27

Catalyst amount: 25 mg; temp: 60 ^{0}C; TBHP: 2 mL

Recycle study

Recycle studies similar to that mentioned in chapter 1 were carried out and same conversion and selectivity for the products are obtained even after multiple cycles (Table 10) indicating that the catalyst remains stable during the course of the reaction and that it can be reused for multiple times.

Table 10. Recycling of catalyst

Catalyst	% Conversion	% Selectivity	
		Benzaldehyde	Styrene-oxide
$PW_{11}Cu/Al_2O_3$	63	60	19
R_1-$PW_{11}Cu/Al_2O_3$	63	60	20
R_2-$PW_{11}Cu/Al_2O_3$	62	60	20
R_3-$PW_{11}Cu/Al_2O_3$	61	61	20

Catalyst amount: 25 mg; Time: 16 h Temp: 60 ^{0}C; TBHP: 2 mL

Characterization of regenerated catalyst

The regenerated catalyst was characterized by FT–IR, FT–Raman as well as powder XRD. Regenerated $PW_{11}Cu/Al_2O_3$ shows the same FT – IR bands as that of the fresh one (Table 11), indicating that the structural morphology of the catalyst remains intact even after the completion of the reaction.

Table 11. FT-IR frequencies of fresh and regenerated $PW_{11}Cu/Al_2O_3$

FT-IR Frequencies (cm^{-1})	P–O	W=O	W–O–W	Cu–O	O–H	H–O–H	O–H–O
$PW_{11}Cu/Al_2O_3$	1099 1064	-	-	-	3437	1627	-
Rec. $PW_{11}Cu/Al_2O_3$	1101 1067	-	-	-	3443	1604	-

Powder XRD of fresh and recycled $PW_{11}Cu/Al_2O_3$ is shown in figure 17. The dispersed spectra is retained in case of recycled catalyst indicating that the catalyst remains dispersed during the course of the reaction an also after recycling.

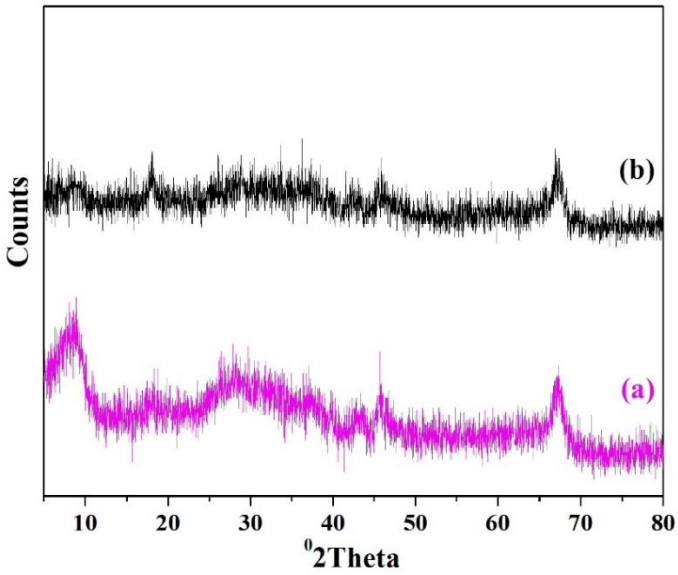

Figure 17. Powder XRD of (a) Fresh and (b) recycled $PW_{11}Cu/Al_2O_3$

Summary

- Wet impregnation technique was successfully implemented to support $PW_{11}Cu$ on to neutral alumina and further characterizations confirmed intact structure, homogeneous dispersion as well as strong chemical interactions between $PW_{11}Cu$ and the support.
- $PW_{11}Cu/Al_2O_3$ showed better catalytic activity compared to $PW_{11}Cu$ for the oxidation of styrene with higher selectivity for benzaldehyde and substantially higher TON. Unfortunately, cis-cyclooctene did not show good conversion and hence, was not continued.
- Control experiments confirmed that the synergic effect between the active species and the support is essential for the higher catalytic activity, and substantially lower activation energy of $PW_{11}Cu/Al_2O_3$ compared to $PW_{11}Cu$ further affirmed the superiority of supported catalyst.
- The catalyst was recycled and reused up to three cycles with negligible loss in activity and characterization of regenerated catalysts confirmed stability of structure.

Comparison of $PW_{11}Cu/ZrO_2$ and $PW_{11}Cu/Al_2O_3$ – effect of support

Oxidation of styrene

Oxidation of styrene over both the supported catalysts was carried out under same reaction conditions and the results are presented in table 12. It is seen that Alumina is better support than Zirconia, may be due to the nature of support. Alumina contains Lewis acidic sites in the form of aluminium. The formed intermediate (less nucleophilic in nature) is able to desorb faster from alumina supported $PW_{11}Cu$, and hence gives higher conversion as well as higher selectivity for benzaldehyde, the complete oxidation product.

Table 12. Oxidation of styrene over $PW_{11}Cu/ZrO_2$ and $PW_{11}Cu/Al_2O_3$

Catalyst	% conversion	% selectivity		Turn Over Number (TON)
		Styrene-oxide	Benzaldehyde	
$PW_{11}Cu/ZrO_2$	44	44	37	2309
$PW_{11}Cu/Al_2O_3$	63	19	60	3306

Catalyst amount-25 mg (active amount of $PW_{11}Cu$-6.25 mg); TBHP – 2 mL; Temperature–60 ^{0}C; Time–16h

References

[1] A. Patel and S. Pathan, Industrial & Engineering Chemistry Research, 2, 732-740, (2012).

[2] J. North, O. Poole, A. Alotaibi, H. Bayahia, E. F. Kozhevnikova, A. Alsalme, M. R. H. Siddiqui and I. V. Kozhevnikov, Applied Catalysis A: General, 16-24, (2015).

[3] L. Hong, P. Win, X. Zhang, W. Chen, H. N. Miras and Y.-F. Song, Chem. Eur. J., 32, 11232-11238, (2016).

[4] K. Parida, A. C. Pradhan, J. Das and N. Sahu, Mater. Chem. Phys., 1, 244-248, (2009).

[5] P. Colomban, J. Mater. Sci. Lett., 12, 1324-1326, (1988).

[6] S. Thanasilp, J. W. Schwank, V. Meeyoo, S. Pengpanich and M. Hunsom, J. Mol. Catal. A: Chem., 49-56, (2013).

[7] A. Kurhade and A. K. Dalai, Asia-Pacific Journal of Chemical Engineering, 6, e2249, (2018).

[8] A. Patel and A. Patel, RSC Adv., 3, 1460-1471, (2019).

[9] Y. Shen, P. Jiang, P. T. Wai, Q. Gu and W. J. C. Zhang, Catalysts, 1, 31, (2019).

[10] Y. Liang, C. Yi, S. Tricard, J. Fang, J. Zhao and W. Shen, RSC Adv., 23, 17993-17999, (2015).

[11] R. Sadasivan, A. Patel and A. Ballabh, Inorg. Chim. Acta, 345-353, (2019).

CONCLUSIONS

- Mono-copper substituted phosphotungstate was successfully supported on two supports, hydrous zirconia and neutral alumina by wet impregnation. The retention of structure as well as interactions was confirmed by various spectral techniques.
- Control experiments confirmed that increase in the % conversion of styrene as well as selectivity of styrene-oxide is due to the synergic effect of the active species ($PW_{11}Cu$) and the supports.
- The supported catalyst showed better catalytic activity as well as lower Ea as compared to the unsupported one for the oxidation of styrene, which showcased the superiority of supported catalyst.
- While $PW_{11}Cu/ZrO_2$ showed higher conversion in case of cis-cyclooctene oxidation, $PW_{11}Cu/Al_2O_3$ did not give good results for the same, in the present system. This is attributed to the nature of support, signifying the role of support in the catalytic activity.
- The catalyst was recycled and reused up to three cycles with negligible loss in catalytic activity, and can also be extended to further catalytic cycles.